FULL ARTICLE

Fouling of Nuclear Steam Generators: Fundamental Studies, Operating Experience and Remedial Measures Using Chemical Additives

C.W. Turner*

Atomic Energy of Canada Limited, Chalk River Laboratories, Chalk River, Ontario, Canada, K0J 1J0

Article Info
Keywords: fouling; steam generator; deposit; dispersant; filming amine
Article History: Article Received April 16, 2013, Accepted June 17, 2013, Available on-line July 12, 2013
DOI: http:dx.doi.org/10.12943/ANR.2013.00007

*Corresponding author: (613) 584-3311, turnerc@aecl.ca

Fouling remains a potentially serious issue that if left unchecked can lead to degradation of the safety and performance of nuclear steam generators (SGs). It has been demonstrated that the majority of the corrosion product transported with the feed water to the SGs accumulates in the SG on the tube-bundle. By increasing the risk of tube failure and acting as a barrier to heat transfer, deposit on the tube bundle has the potential to impair the ability of the SG to perform its two safety-critical roles: provision of a barrier to the release of radioactivity from the reactor coolant and removal of heat from the primary coolant during power operation and under certain post accident scenarios. Thus, it is imperative to develop improved ways to mitigate SG fouling for the long-term safe, reliable and economic performance of nuclear power plants (NPPs). This paper provides an overview of our current understanding of the mechanisms by which deposit accumulates on the secondary side of the SG, how this accumulation affects SG performance and how accumulation of deposit can be mitigated using chemical additives to the secondary heat-transport system. The paper concludes with some key questions that remain to be addressed to further advance our knowledge of deposit accumulation and how it can be controlled to maintain safe, economic performance of nuclear SGs.

Nomenclature

Upper Case

A	Surface area of SG tube-bundle (m^2)
A_{site}	Surface area of a bubble nucleation site (m^2)
BD	Blow down mass flow rate (kg/s)
C	Mass fraction of material in suspension (or solution) (kg/kg)
E	Activation energy (Joule/mole)
D	Pipe diameter (m)
D'	Particle diffusion coefficient (m^2/s)
F	Force (Nt)
K	Mass transfer velocity (m/s)
M	Mass of liquid in a Recirculating Steam Generator (kg)
N_{active}	Active nucleation site density (m^{-2})
R	Universal gas constant (Joule/mole K)
Re	Reynolds Number = (DU/ν)
Sc	Schmidt Number = (ν/D')
T	Temperature (K), (^oC)
U	Velocity (m/s)
U*	Friction velocity (= 0.199U/Re0.125) (m/s)

Lower Case

h	Heat-transfer coefficient ($W/m^2\ ^oC$)
m	Deposit mass (kg/m^2)
m'	Number of turbulent bursts per unit area (m^{-2})
t	Time (s)

Subscript

a	Attachment
b	Bulk
d	Deposition (or deposit)
D	Drag
f	Fluid
L	Lift
p	Particle
r	Removal
s	Surface
t	Transport

Greek

ρ	Density (kg/m^3)
ν	kinematic viscosity (m^2/s)

1. Introduction

The function of the steam generator (SG) in an indirect cycle nuclear-power plant (NPP) is to generate steam from the nuclear heat produced by fission reactions in the core during operation at power, and to act as a heat sink to remove decay-heat from fission products during both normal reactor shut down and for a post accident scenario in the event that reactor-core cooling has been impaired. Situated at the boundary between the nuclear (radioactive primary coolant system) and conventional (non-radioactive secondary coolant system) sides of the plant, the SG plays two safety-critical roles:

1. Provides a barrier to prevent the release of radioactivity from the primary reactor coolant to the secondary coolant where it can be released to the environment; and,
2. Removes heat from the primary coolant to the secondary coolant to maintain a safety margin during power operation and some post accident scenarios.

Thus, the integrity of the SG and its internal components is vital for assuring both the safety and the performance of the NPP [1, 2].

Despite improvements in materials, designs and water chemistry, degradation affecting the safety and performance of the SG continues to be a major concern within the nuclear industry [3, 4]. For example, perforation of the SG tube wall as the result of either outside-diameter stress corrosion cracking (ODSCC), fretting wear or high-cycle fatigue provides a leakage path for radioactive, primary coolant to the secondary side where it can subsequently be released to the environment. Additional inspection and repair activities to ensure the integrity of the SG tube-bundle have a negative economic impact on plant performance, and lead to additional radiation exposure to plant personnel. Every SG design has a multitude of crevices at the tube/tube-support intersections which, when partially filled with deposit, become concentration sites for impurities which, in turn, increases the risk of ODSCC. Understanding the relationships between deposit accumulation, the development of aggressive chemistry environments and the impact of these environments on the risk of ODSCC must remain a key focus area for the industry, especially in light of the 60-plus year lifetimes that are now expected for SGs to meet the economic needs of NPPs. Recent tube failures in some Electricité de France (EdF) plants were caused by high-cycle fatigue related to flow re-distribution and tube lock up in the tube-support structure of the SG. Remedial measures included chemical cleaning of all the affected SGs in the fleet at significant cost to the utility. The accumulation of deposit on the tube-bundle[1] and tube-support[2] structure is also a concern with respect to its impact on the thermal-hydraulic performance of the SG. Heavy deposit on the tube-bundle has contributed to a loss of thermal performance during power operation at some NPPs as well as other operational problems, such as density-wave oscillations in the SGs, which could only be remediated by chemical cleaning to remove the accumulated deposit.

Almost without exception, the degradation that affects the safety and performance of the SG is related in one way or another to the accumulation of deposit on various components on the secondary-side of the SG, e.g., the tube-bundle, tube-support structure, tube-sheet and steam separators. A corollary of this statement is that a properly designed SG should not fail by any of the above-mentioned degradation mechanisms provided that the SG remains clean, i.e., free of deposits. Thus, the key to mitigating degradation of the SG is the ability to mitigate the accumulation of unwanted deposit, or fouling, of the surfaces of critical components within the SG.

This paper provides an overview of the current understanding of the mechanisms by which deposit accumulates on the secondary side of the SG, how this accumulation affects SG performance and how accumulation of deposit can be mitigated using chemical additives to the secondary heat transport system. The paper concludes with some key questions that remain to be addressed to further advance our knowledge of deposit accumulation and how it can be controlled to maintain safe, economic performance of nuclear SGs.

2. Nuclear Steam Generators: Design and Operating Experience

2.1 Nuclear SG Design

The SGs used in pressurized-water reactors (PWRs) are large tube-in-shell heat exchangers that use heat from the primary reactor-coolant system to generate steam in the secondary system to drive the turbine generators. Two designs of SG in use at NPPs in Asia, Western Europe and the Americas are the vertical U-tube Recirculating Steam Generator (RSG) and the vertical Once-Through Steam Generator (OTSG) illustrated in Figures 1 and 2, respectively. Russian-designed pressurized water reactors use a horizontal SG design, as shown in Figure 3, which has been implemented in plants built in Russia and in Eastern Europe [5]. The SGs at AECL's Nuclear Power Demonstration (NPD) plant, which was commissioned in 1962, were also a horizontal design.

[1] Precipitation fouling on the inside surface of the tube bundle as a result of the use of carbon steel for the feeder pipes and reactor coolant piping also leads to a loss of thermal performance in CANDU SGs. Precipitation fouling from the primary coolant will not be reviewed in this report.

[2] The one obvious exception is fretting wear associated with an improperly designed tube support structure, which can cause high tube-failure rates resulting from an excessively high fretting wear rate early in the life of the SG.

For all nuclear SGs, the primary reactor coolant flows on the inside of the SG tubes and boils water, i.e., the secondary coolant, on the outer surface, or shell side, of the tubes. In the vertical RSG design, feed water enters the SG either through a feed ring at the top of the tube-bundle or via an integral preheater located at the base of the cold-leg, as shown in Figure 1. The feed water is mixed with separated water from the steam separators, and then flows up through the tube nest where steam is generated. About 25 wt.% of the water is converted to steam on a single pass through the tube nest. The remainder is separated from the steam-water mixture in the steam separators and recirculated through the tube nest via the down comer, while the separated steam is sent to the turbine generator. A small flow of water known as blow down, corresponding to 1% or less of the main steam mass flow rate, is removed from the SGs on a continuous basis to limit the build up of impurities in the recirculating water. In the OTSG design (see Figure 2), the secondary water enters the SG at about the tenth tube-support plate (TSP) and is heated while it drains via the down comer to the tube-sheet, where it enters the tube nest. The OTSG is divided into two regions: the boiling region between the tube-sheet and the tenth TSP where the feed water is converted entirely to steam, and the super-heater section above the tenth TSP, where the steam is superheated before being sent to the turbine generator. In both the RSG and OTSG designs, after passing through the turbine generator, the steam is condensed and returned to the SGs via a series of feed water heaters that are heated using steam extracted from the high-pressure and low-pressure turbines.

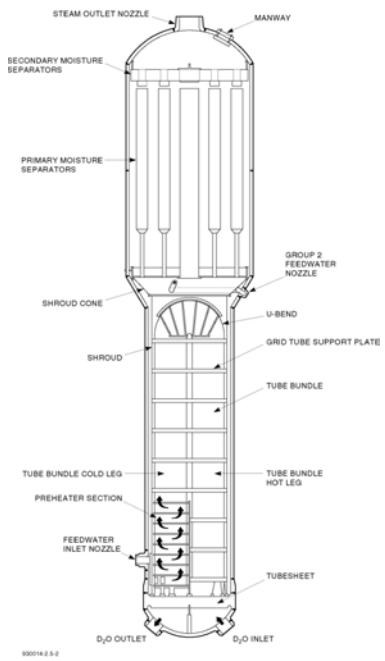

FIGURE 1: Illustration of a vertical U-tube Recirculating SG (RSG) for a CANDU 6 NPP.

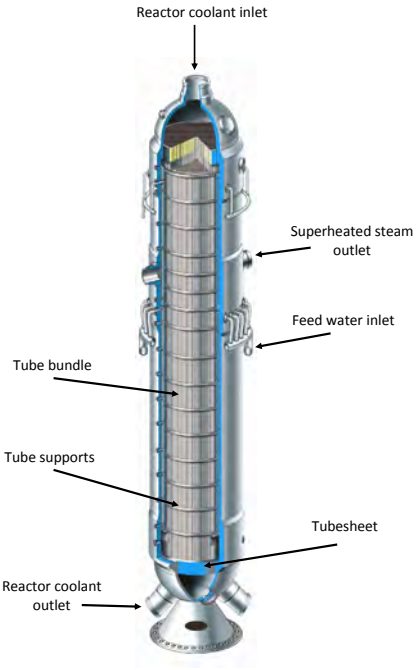

FIGURE 2: Illustration of a vertical Once Through SG (OTSG) (courtesy of Babcock and Wilcox).

For the horizontal SG (see Figure 3), primary coolant enters the SG via a vertical header, flows through the horizontal SG U-tube-bundle and exits via a second vertical header. The inlet and outlet primary-coolant headers perforate the SG shell near the middle of the shell. Feed water is supplied to the shell-side of the tube-bundle at the middle of the tube-bundle via perforated piping under a perforated sheet. The tube-bundle is entirely submerged in the secondary coolant.

2.2 Transport of Corrosion Products to the SGs

An illustration of a typical feed-water-heating system used at a CANDU pressurized heavy-water reactor (PHWR) is shown in Figure 4. The materials of construction for the feed-water-heating system are typically carbon steel for the piping, condenser and heater shells and tube-sheets, stainless steel or titanium for the condenser tubes, stainless steel for the low-pressure (LP) feed water heater tubes and carbon steel for the high-pressure (HP) feed water heater tubes. The condensate that drains from the heater shells is pumped back to either the deaerator storage tank (from the HP heaters and steam re-heater drains) or to the condenser (from the LP heaters) to maximize system thermal efficiency. While maximizing thermal efficiency, this design ensures that corrosion products that are removed from the

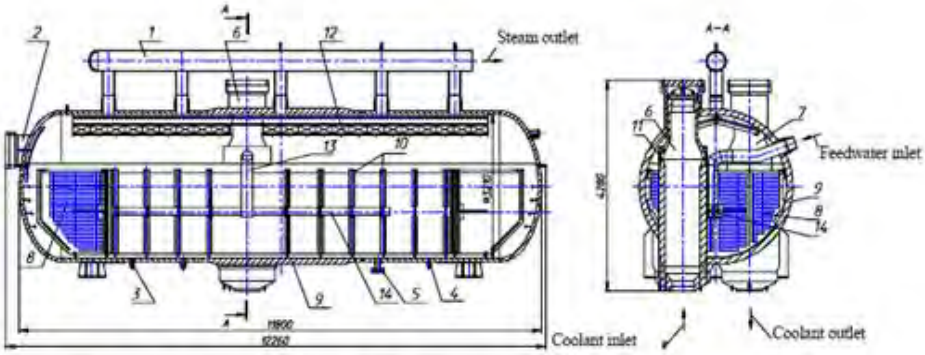

Structure of steam generator PGV-440:
1 – steam header, 2 – hatch-manhole; 3, 4 – blowdown pipe sleeves; 5 – drainage pipe sleeve; 6, 7 – "hot" and "cold" collectors; 8 – heat exchanging tubes; 9 – steam generator vessel; 10 – heat exchanging tube bundle supports; 11 – protective housing; 12 – separation blinds; 13 – feed water supply tube; 14 – feed water distribution collector

FIGURE 3: Illustration of a horizontal SG (OKB Gidropress [5]).

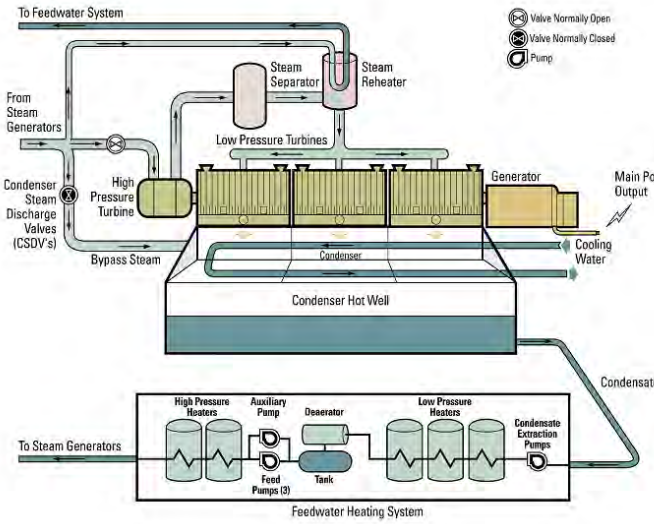

FIGURE 4: Illustration of a typical feedwater heating system in a CANDU pressurized heavy water reactor.

surfaces of carbon-steel piping and components during operation are ultimately transported with the feed water to the SGs where they can accumulate on internal structures such as the tube-bundle, tube-support structure and the tube-sheet. Experience has shown that unless otherwise removed, the accumulation of corrosion products on these internal surfaces will eventually lead to degradation of the safety and performance of the SGs [6].

The rates of iron transport at various locations of the feed water heating systems of PWRs have been thoroughly investigated by determining the quantity of corrosion product that accumulates on a filter with a nominal pore size of 0.45 μm followed by a cation exchange membrane. These studies have concluded that a majority of the iron (> 90% of the mass) is transported to the SGs in the form of suspended particulate material, with the remainder being a combination of dissolved iron and iron in colloidal form that passes through the 0.45 μm sample filter [7, 8].

Mossbauer analyses of the corrosion products in filtered water removed from various locations of the condensate/feed water systems of PHWRs find primarily magnetite, hematite and lepidocrocite, with goethite appearing in some samples as a minor constituent [7, 9]. Similar analyses of the material filtered from the condensate/feed water system of PWRs find magnetite and hematite as major constituents, with relatively less lepidocrocite and more goethite than is generally found at PHWRs [9, 10]. Iron transport investigations conducted at RBMK and VVER plants also report magnetite, hematite and lepidocrocite as being the major constituents of the corrosion products filtered from the hot-water systems at these plants [11].

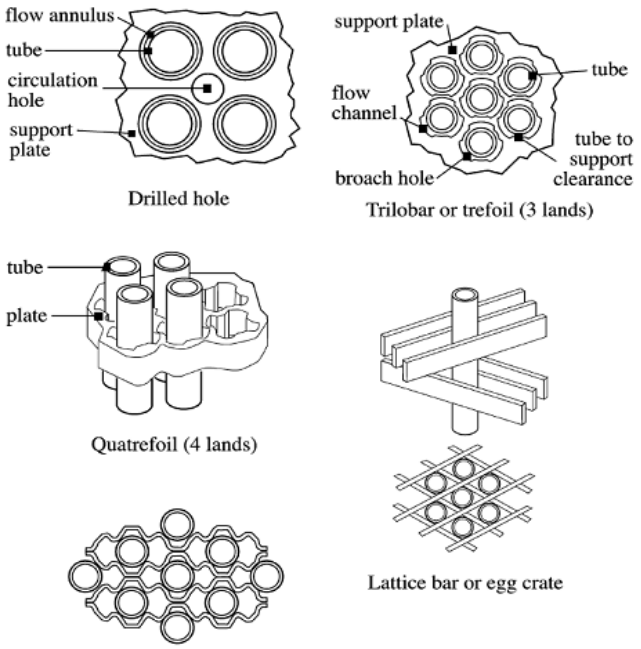

FIGURE 5: Illustrations of different tube support designs used in nuclear SGs [31].

Although the results from corrosion product transport investigations at operating NPPs appear to be relatively consistent from one plant to another, how representative the samples are is still open to question. For example, long sample lines (up to 100 m in length) are used to deliver the sample stream to a centralized collection point, and almost invariably the sample is cooled before passing through the 0.45 μm filter to collect the suspended particles. Sampling nozzles have not necessarily been designed to ensure that the fluid entering the nozzle has the same velocity as the main stream, i.e., to ensure isokinetic sampling [12, 14, 15]. Thus, corrosion products sampled using existing sampling systems at NPPs are subject to the following uncertainties:

1. Precipitation of dissolved iron-on cooling will result in the concentration of dissolved iron in the system being under estimated and the concentration of suspended particulate being over-estimated. Precipitation on cooling may also affect the particle-size distribution of the filtered sample,

2. Anisokinetic sampling could influence the measured concentration and bias the particle size distribution of suspended material in the sample stream. Deposition and removal within the sample lines may affect the concentrations of both dissolved (by dissolution of existing deposit within the sample line) and suspended corrosion product.

Although the uncertainties introduced by anisokinetic sampling can be significant for an aerosol [13], the importance of matching the sample and fluid velocities diminishes when sampling for suspended material in a liquid because the higher viscosity of the fluid makes it more likely for the particle to follow the fluid streamline. For example, simulations of the particle collection efficiency for 1 μm particles of magnetite suspended in 300 °C water and in steam show that the sampling velocity has no discernable influence on the results for velocities ranging from 25% to 175% of the isokinetic velocity for the aqueous system, but results in errors of up to 25% when sampling for those same particles entrained in steam [16]. As expected, the deviations become more significant with increasing particle size. Measurements of iron transport in the feed water at the Winfrith[3] experimental Steam Generating Heavy Water Reactor (SGHWR) using capillary lines and isokinetic sampling found that dissolved iron constituted only ~ 1 % of the mass of iron transported between the high-pressure feed-water heaters, and ~ 0.5 % of the mass of iron transported in the final feed water [14]. Measurements as a function of sample fluid velocity showed an absence of bias for fluid velocities between 75% and 125% of the isokinetic velocity. Deviations of +22% and -27% were reported for velocities of 30% and 200% of the isokinetic velocity, respectively. A study comparing hot filtration with filtration at ambient temperature using Ag and cellulose membrane filters, respectively, found no significant difference in particle size between the high-temperature and ambient-temperature samples [17]. Interestingly, the concentrations of dissolved iron were relatively consistent from one sample to the next[4], whereas the concentrations of filterable iron were three to six times lower in the samples filtered at ambient temperature compared to hot filtration. Although there are insufficient data to make a strong conclusion, particle deposition on the cooler may account for the lower concentration of filterable material in the sample filtered at ambient temperature[5].

A sampling system to permit isokinetic sampling and hot filtration of particulates in the reactor coolant system of a PWR has been designed and commissioned [18] to provide representative samples to estimate particulate concentrations in the reactor coolant system at Diablo Canyon. The technology does not look complicated, and it would be beneficial if a similar system were implemented to collect more representative samples of corrosion products suspended in the feed-water systems of NPPs.

Based on measurements of corrosion-product transport during steady operation at full power, it is estimated that from 25 to 50 kg of iron are transported to the SGs per

[3]The SGHWR was one of several experimental research reactors built at the Winfrith site in the United Kingdom.
[4]The data base from this study is small: three samples filtered hot, of which one was compromised by a torn membrane, and two samples filtered cold. The results from the torn membrane were not used for this analysis.
[5] Particle transport down a temperature gradient leading to deposition on a cold surface is known as thermophoresis, and is discussed later in this review.

year for a plant operating with between 1 and 2 μg/kg of iron in the feed water [6]. An equivalent amount of iron can be transported to the SGs during a single-crud burst during start-up, although this amount can be reduced by circulation and filtration of the secondary coolant prior to heat-up [19]. For comparison, chemical cleaning of the SGs at Point Lepreau Nuclear Generating Station (PLNGS) [20] resulted in the removal of 830 kg of iron from four SGs after 11.7 effective full power years (EFPY) of operation, which corresponds to an annual accumulation rate of 71 kg of iron per year of full-power operation. Chemical cleaning at Gentilly 2 NGS [21] removed 950 kg of iron from four SGs after approximately 18 EFPY of operation, corresponding to an annual accumulation rate of 53 kg iron per year of full-power operation. Most of this deposit would have been removed from the tube-bundle, since both plants water lance the tube-sheets of each SG about once every four years resulting in the removal of about 10 to 20 kg of tube-sheet deposit per campaign.[6]

2.3 Impact of Fouling on the Safety and Performance of Nuclear SGS

Fouling was originally a descriptive term used in the oil industry to refer to the accumulation of undesirable deposit on heat-exchanger surfaces that increases the resistance to heat transmission [22]. The accumulation of corrosion products on the internal surfaces of a nuclear SG can severely degrade SG performance and increase the risk of materials degradation as a result of:

1. Formation of a resistive layer of deposit on the tube surface that could reduce the rate of heat-transfer from the primary to the secondary coolant and decrease the safety margin,
2. Accumulation of ionic impurities to form-concentrated solutions that are aggressive to tube integrity under thick deposits or in deposit filled crevices between the tubes and the tube-support structure,
3. Restriction of the movement of the tubes caused by deposit build-up on the tube-support structure; tube "lock up" leading to high-cycle fatigue,
4. Blockage of the flow passages of the tube-support structure, resulting in several operational and materials degradation problems discussed below, and,
5. Accumulation of a thick sludge pile on the tube-sheet that becomes increasingly consolidated with time, with deleterious consequences for tube integrity.

The formation of a layer of corrosion product on the boiling-side of the SG tube has two separate effects on heat-transfer. The outer porous layer provides additional sites for bubble nucleation and, thus, reduces the wall superheat required for bubble nucleation. This is manifested by an improvement in heat-transfer as the bare tube surface becomes covered with a thin layer of porous deposit. As deposits grow thicker, however, they develop a layered structure, with a dense inner layer that is resistive to heat-transfer and a porous outer layer that enhances heat-transfer [23]. The net result is that many RSGs show a net improvement in thermal performance during the first few years of operation, followed by a steady deterioration in thermal performance as thicker deposit grows onto the tube-bundle [24]. Other factors, such as changes in primary and secondary coolant flow rates, separator fouling and SG divider plate leakage to name a few, have also been shown to contribute to the degradation of SG thermal performance, and so a systematic approach must be taken to quantify all contributions to thermal performance degradation before taking any remedial action [25, 26].

The accumulation of deposit on the heat-transfer surface also raises the risk of under-deposit corrosion, especially in crevice regions at the tube-sheet, top of the sludge pile and at the tube/tube-support intersections [27] where high concentrations of impurities can accumulate during power operation through a process known as "hideout" [28, 29]. Hideout is driven by the evaporation of liquid within the pores of the deposit. As the liquid within the pores evaporates, it is replaced by fresh solution that is drawn into the deposit by capillarity. The fresh solution brings with it additional non-volatile ionic species, thus increasing the concentration of the solution in the pores. As the concentration of the solution increases, selected compounds will precipitate, depending on their solubility. The pH of the solution that remains in equilibrium with the precipitate is determined by the relative concentrations of ionic species that remain in solution. Thus, the pH in fouled crevice regions and within the pores of thick deposits is not determined by the amine that is added for pH control in the steam cycle. It is ultimately determined by the relative concentrations of soluble impurities that are transported to the SG with the feed water and by the solubilities and compositions of those compounds that precipitate in the crevices under boiling heat-transfer conditions. Electric Power Research Institute (EPRI) and AECL have developed codes to predict the high temperature crevice pH that results from hideout and precipitation of non volatile soluble ionic species based on equilibrium models of crevice chemistry.

This information, combined with measurements of the electrochemical corrosion potential (ECP) of SG tubes in various crevice environments, has been used to establish two-dimensional maps of pH and ECP at 25, 150 and 300 °C where the risk of localized crevice corrosion and pitting of SG tubes is at a minimum [30].

Accumulation of deposit on the SG tube-support structure can lead to both operational problems affecting the

[6] A pair of SGs are water lanced to remove tube-sheet deposit every two years, which means that the tube sheet of each SG is water lanced once every four years.

performance of the SG and to degradation of the support structure and the SG tubes. Examples of common tube-support designs used in nuclear SGs are shown in Figure 5 [31]. The trefoil and quatrefoil tube-support plate (TSP) design designs are particularly susceptible to deposit accumulation within the flow-holes of the TSP, which causes an increase in the pressure drop across the TSPs. Flow blockage tends to be higher on the hot-leg side of the SG compared to the cold-leg, and increases in the boiling zone with increasing steam quality. The increased pressure drop across the TSPs has led to flooding of the aspirator ports in OTSGs designed by Babcock and Wilcox [32, 33, 34] and to the onset of density wave oscillations in RSGs of both the Westinghouse [35] and the Babcock and Wilcox [36, 37] designs[7]. In both cases, the short-term remedial solution was to operate the plants at reduced power until such time as the deposit could be removed from the flow passages of the TSPs by either water-slap or chemical cleaning. The SGs at Gentilly-2 also showed early signs of level oscillations prior to chemical cleaning [21].

Blockage of the quatrefoil TSPs in SGs at the Cruas NPP did not lead to density-wave oscillations, but instead to a re-distribution of flow in the upper-bundle region that caused flow-induced vibration (FIV) that was outside of the design basis of the SG. FIV ultimately resulted in failure of some tight-radius SG tubes by high cycle fatigue [38], [39]. The problem was exacerbated somewhat by the SG design which included a tube-free region in the centre of the bundle. Interestingly, the heavy TSP blockage did not manifest itself in the onset of a density-wave oscillation, as observed in other RSGs with blocked trefoil or quatrefoil TSPs. However, thermal-hydraulic analyses concluded that the SGs were susceptible to the onset of a density-wave oscillation in response to certain transients, such as a 10% step in reactor power. A subsequent investigation concluded that the tube failures were caused by a combination of: 1) Blockage of the flow-holes of the quatrefoil TSPs that caused the steam/water mixture to be re-directed towards tubes near the centre of the bundle with small-radius bends, and 2) Tube lock-up, resulting from heavy fouling of the tube-TSP intersections, which increased the local stress intensity of the tubes.

Partial blockage of the trefoil TSPs on the hot-leg and extensive degradation of the carbon-steel TSPs on the cold-leg was identified in 2004 by a visual inspection of the SGs at the Embalse NPP [40, 41]. The degradation on the cold-leg was attributed to flow-accelerated corrosion (FAC) of the low chromium (0.07 to 0.08 wt. %) carbon steel TSPs. Partial blockage of the trefoil TSP on the hot leg, which led to a re-distribution of the riser flow and relatively high fluid velocity on the cold-leg, was identified as a contributing factor. FAC was also identified as the cause of extensive degradation of the carbon steel trefoil TSPs at Unit 8 of the Bruce NPP, with the low chromium content of the carbon steel (0.03 to 0.04 wt. %) and relatively high local fluid velocity cited as exacerbating factors [42]. The highest damage rates at the Bruce Unit 8 SGs were found on the periphery of the hot leg. Although partial blockage of the TSPs at Bruce has been observed, it was not cited as a possible contributing factor.

3. Particulate fouling: Modelling and Experiments

3.1 Fouling – The Fundamental Steps

Epstein has outlined five fundamental steps involved in the process of fouling of a pipe wall or surface [43]:

1. Initiation (incubation period, surface conditioning, crystal nucleation),
2. Transport (mass transfer from the bulk to the surface),
3. Attachment (attachment of the foulant to the surface),
4. Removal (release, re-entrainment, detachment of the foulant from the surface), and,
5. Aging (dehydration, recrystallization, changes of physical or chemical properties of the accumulated deposit with time).

Each of these steps will be discussed in turn in the following sections. Please refer to the Nomenclature section for a complete listing of the symbols used in the equations.

3.1.1 Initiation

Initiation is associated with phenomena taking place on a wall or substrate that preclude a more rapid rate of fouling and is often but not always observed with precipitation fouling and biofouling, where the initiating phenomena could be nucleation of crystals and adsorption of polymeric substances important for the growth of microorganisms, respectively. There is no initiation step observed with particulate fouling, and so initiation will not be considered further in this report.

3.1.2 Transport

Transport is the best understood of the fundamental steps of the fouling process, where the mass flux of material transported from the bulk fluid to the wall is given by:

$$m_t = \rho_f K_t (C_b - C_s) \quad (1)$$

A thorough review of investigations into the mechanism of particle transport can be found in Reference [44].

For a suspension of colloidal particles in turbulent flow, Metzner and Friend derived an expression for the transport velocity of colloidal particles that simplifies to [45]:

$$K_t = U^* / (11.8 \cdot Sc^{2/3}) \quad (2)$$

[7]Density-wave oscillations can occur in a system if there is a higher pressure drop in the two-phase flow region than in the region where the flow is single-phase. Density-wave oscillations in an RSG manifest themselves as oscillations in the water level in the SG.

Using an entirely different approach, Cleaver and Yates [46] derived a similar expression with the factor 11.9 in the denominator instead of 11.8.

Equations (1) and (2) apply to particle sizes and fluid velocities that are low enough that inertial effects are not important, i.e., the particle dimensionless relaxation time, t_p^+, is < 0.1, where [46],

$$K_t = U^* / (11.8 \cdot Sc^{2/3}) \quad (3)$$

A number of expressions and approaches have been developed to predict the transport velocity of particles in the inertial transport regime, i.e., for $t_p^+ > 0.1$ [46, 47, 48, 49, 50, 51]. Each of these methods predict a rapid increase in the dimensionless deposition velocity (K_t/U^*) in the range $0.1 < t_p^+ < 10$, followed by a region where the dimensionless deposition velocity is independent of t_p^+. Although the predicted deposition velocities are in reasonably good agreement with data for aerosols, they tend to overestimate the transport velocity by two to three orders of magnitude when compared to deposition data for aqueous suspensions of particles [44, 52].

3.1.3 Attachment

Under some circumstances, the rate at which particles deposit onto a wall in an aqueous medium is observed to be less than the rate at which particles are transported from the bulk to the wall region. This has been accounted for by the introduction of an additional step in the fouling process known as attachment, which acts in series with transport to determine the overall rate at which particles deposit onto a substrate from a flowing suspension [53, 54]. Treating transport and attachment as two steps in series, the deposition velocity, K_d, is written:

$$1/K_d = 1/K_t + 1/K_a \quad (4)$$

where,

$$K_a = K_0 \exp(-E/RT) \quad (5)$$

and the rate of particle deposition is given by:

$$\dot{m}_d(t) = \rho_f K_d (C_b - C_s) \quad (6)$$

The rate of deposition can be limited by either the rate of particle transport from the bulk fluid to the wall or by the rate of attachment to the wall, whichever is smaller. Thus, for $K_t << K_a$, the rates of particle transport and attachment will be equal when $C_s \rightarrow 0$. In this case, the transport limited deposition rate will be given by:

$$\dot{m}_d \cong \rho_f K_t C_b \quad (7)$$

Alternatively, for $K_t >> K_a$, the rates of particle transport and attachment are balanced for $C_b \cong C_s$, and the attachment limited deposition rate will be given by:

$$\dot{m}_d \cong \rho_f K_a C_b \quad (8)$$

The activation energy, E, in Equation (5) has its origin in the forces of interaction between the particle and the substrate, as discussed below. Examples of particle deposition limited by either transport or attachment are discussed in Section 3.3.1.

The surface interaction forces that come into play when a particle comes into close proximity to a substrate are described by the Derjaguin-Landau-Verwey-Overbeek theory of colloid stability, which is well described in numerous textbooks on colloid science [55], and so will not be discussed further in this paper. The net result of these forces of interaction is that once the particle has been transported to the vicinity of the substrate, it will be subjected to either a net force of attraction or a net force of repulsion, depending on the relative sign of the respective surface charges.[8]

Water has been called the "universal solvent", and it is well known that materials in an aqueous medium develop a surface charge as the result of chemical equilibria between ionic species in solution and the material itself. The surfaces of corrosion products and Fe-Cr-Ni alloys consist of hydrated metal oxides, which become charged as the result of preferential adsorption of H^+ and OH^- ions, which can be simply represented by the following reactions:

$$\rangle M(OH)_2 + H_2O \Leftrightarrow \rangle M(OH)(OH_2)^+ + OH^- \quad (9)$$

$$\rangle M(OH)_2 + H_2O \Leftrightarrow \rangle M(OH)O^- + H_3O^+ \quad (10)$$

where $>M(OH)_2$ represents a hydrated oxide on the surface. It is clear from these equations that, in the absence of other equilibrium reactions, which may influence the surface

[8]The net force between a particle and substrate is equal to the sum of the van der Waals dipole-dipole interaction between the two bodies (which is always positive, or repulsive, in water) and a force of electrochemical origin which is positive (repulsive) if the two surfaces are of similar sign of charge, and negative (attractive) if the two surfaces are of opposite sign of charge.

charge, the sign of the surface charge of hydrated metal oxides will be determined by the pH. This dependence has been confirmed by numerous measurements reported in the literature [56]. The pH at which the net surface charge is zero is called the Point of Zero Charge (PZC), and the corresponding pH at which the potential at the plane of shear between a surface and the aqueous medium (the zeta potential) is zero is called the Isoelectric Point (IEP).[9]

For pH < PZC (IEP), the surface charge (zeta potential) will be positive. Correspondingly, for pH > PZC (IEP), the surface charge (zeta potential) will be negative. Therefore, if the pH of the medium is at a value that is between the PZCs (IEPs) of the particle and the substrate, the surfaces will be oppositely charged and the net force between them will be attractive. For pH outside of this regime, the surfaces will be similarly charged and the net force between the particle and the substrate will be repulsive.

3.1.4 Removal

Particles that have been transported to the wall and become attached do not necessarily remain there forever because they will continue to be acted upon by forces generated by the fluid flow. The hydrodynamics of particle removal in a turbulent flow have been thoroughly reviewed [57], and removal criteria based on particle size, wall-shear stress and the force of adhesion have been postulated.

Particles in steady shear flow are subjected to a drag force acting parallel to the direction of flow [58]:

$$F_D = 8\rho_f \nu^2 (d_p U^*/\nu)^2 \quad (11)$$

and to a lift force acting normal to the direction of flow [59, 60]:

$$F_L = 0.81\rho_f \nu^2 (d_p U^*/\nu)^3 \quad (12)$$

Starting with a flow model based on the theory of "turbulent bursts", Cleaver and Yates derived a similar expression for the lift force as that shown in Equation (12) except with a constant 0.076 [57] instead of 0.81. Regardless, for $(d_p U^*/\nu) < 1$, the particle will be buried deep within the so called "viscous", or laminar, sub-layer[10], and the lift force will be significantly smaller than the drag force. Although drag may cause a particle to roll or slide along the surface, it does not provide a component of force normal to the surface. Nor does it seem capable of moving a particle from the surface into the turbulent flow, as could be imagined for the case where $(d_p U^*/\nu) >> 1$. Thus, for small particles, i.e., $(d_p U^*/\nu) < 1$, the criteria for removal is that the lift force must exceed the force of adhesion holding the particle onto the surface. Assuming that all adhesive forces are proportional to the particle diameter, the criteria for particle removal becomes [57]:

$$(\rho\nu^2/d_p)(d_p U^*/\nu)^3 > \beta \quad (13)$$

where β is inversely proportional to the force of adhesion. For larger particles, i.e., $(d_p U^*/\nu) >> 1$, the drag force plays a more significant role in particle removal and the criteria for removal becomes:

$$(\rho\nu^2/\rho_p)(d_p U^*/\nu)^2 > \beta \quad (14)$$

Cleaver and Yates developed a model of simultaneous deposition and removal of particles whereby particles are transported to a surface by a coherent downsweep of fluid turbulence and are either deposited in that downsweep (or subsequent downsweep) or transported back to the bulk by an outward turbulent burst [61]. The model provides a conceptual way to understand how particles can be simultaneously deposited and removed from a surface. The effect of removal on the overall rate of accumulation of particles onto a surface is given by:

$$N(t) \propto 100\nu m'/U^{*2}(1 - \exp(-U^{*2}t/(100\nu m'))) \quad (15)$$

provided that the lift force generated by a burst is sufficient to overcome the force of adhesion and remove some fraction of the particles. In Equation (15), $100\nu/U^{*2}$ is the time between turbulent bursts and m' is the number of bursts per unit area.

Yung *et al.* compared the predictions of Cleaver and Yates' removal mechanism with measurements of the removal of particles from a substrate by turbulent burst activity, as recorded by high-speed photography [60]. For their investigation, the particle size was such that $0.5 < d_p U^*/\nu < 1.3$. Yung *et al.* found that the initial movement of a particle on a substrate under the influence of turbulent bursts is by rolling or possibly sliding along the surface. The rate of removal observed was not proportional to the rate of turbulent bursts, and the turbulent bursts were not very effective at removing particles buried deep within the laminar sub-layer. The cleaning efficiencies reported by Yung *et al.*, i.e., the fraction of the area under a turbulent burst that is cleaned of particles for a given burst, were very small, ranging from 0.013% to 0.58%.

Although the results of the investigations reported in this section provide good insights into the hydrodynamics of particle removal from substrates, there are too many

[9] The pH that corresponds to the PZC may be different from the pH at the IEP if there are charged species on the surface other than H^+ and OH^-. Although it is important to distinguish between PZC and IEP, this topic is thoroughly discussed in the literature and is outside of the scope of this paper. The parameter of interest for particle deposition is the IEP, which determines whether the particle experiences a force of repulsion or attraction when it arrives within the vicinity of a substrate.

[10] The thickness of the laminar sub-layer in a turbulent flow, where turbulent eddies are rapidly damped by the fluid viscosity, is given by $\nu/U^* < 5$. Thus, for $(d_p U^*/\nu) < 1$, the particles are less than 20% of the thickness of the laminar sub-layer.

uncertainties in the parameters for this to form the basis for a useful predictive theory of particle removal for aqueous systems. Therefore, investigators must resort to an empirical model to take account of the effect of removal on the fouling rate. A common approach is to assume a rate of removal that is proportional to the deposited mass:

$$\dot{m}_r = - \lambda_r m_s (t) \quad (16)$$

Equation (16) is presumed to hold provided a critical threshold for particle removal is satisfied. For example, one could use the criterion that the dimensionless particle Reynolds number, $d_p U^*/\nu$, must be greater than 1 (i.e., the particle size must be greater than 20% of the thickness of the laminar sub layer) for a particle to be removed from the wall by the hydrodynamic forces.

The approximation that the rate of removal remains proportional to the deposited mass once the surface coverage of particles exceeds one monolayer is open to question. Only the outer layer of particles will be fully exposed to the hydrodynamic forces, therefore some adjustment must be made to Equation (16) to account for the fact that particles beneath the outer surface will not be subjected to the full hydrodynamic force. Thus, for $m(t) > m_{monolayer}$, a more realistic expression for the rate of removal once the surface is covered with at least one monolayer of particles is:

$$\dot{m}_r = - \lambda_r f m_{monolayer} \quad (17)$$

where f is a constant of proportionality (assumed to be $\geqq 1$) that depends on the degree to which the deposited particles are bound to one another.

3.1.5 Deposit Aging

Although much attention has been paid to modelling the contributions of transport, attachment and removal to particulate fouling, relatively little attention has been paid to the mechanism of deposit aging, or consolidation, and its effect on fouling behaviour. Consolidation is the process whereby particles become chemically bonded to both the heat-transfer surface and to pre-existing deposit, and is accompanied by an increase in deposit density and strength. It has been demonstrated that consolidation involves the precipitation or re-crystallization of material within the pores of existing deposit [62]. Processes that have been suggested to contribute to consolidation include Ostwald ripening, dissolution and re-precipitation of corrosion product in a temperature gradient and boiling-induced precipitation of dissolved species [63].

Ostwald ripening is the process whereby smaller particles or crystals dissolve and re-precipitate onto the surfaces of larger ones [64]. The process is thermodynamically favoured because it is accompanied by a reduction in surface area and, therefore, of surface energy. Consolidation by dissolution and re-precipitation takes place wherever a deposit resides in a temperature gradient. A gradient in temperature will be accompanied by a corresponding gradient in solubility across the deposit. The net result is that the deposit in the more soluble region will tend to dissolve and re-precipitate within the pores of regions of lower solubility. For deposit composed of material with a retrograde temperature-dependent solubility, the deposit will tend to dissolve at the deposit fluid interface and re precipitate at the heat-transfer surface. This phenomenon has been demonstrated with the precipitation of calcium carbonate from a flowing solution onto a heat-transfer surface [65] and with the precipitation fouling of magnetite onto the inside surface of SG tubes located in the preheater section of a CANDU SG [66], where the deposit porosity at the heat-transfer surface was estimated to be ~ 5%. The third mechanism proposed for consolidation, boiling induced precipitation, will contribute to deposit consolidation on the secondary side of the SG for deposit on the tube-sheet, on the tube-bundle and at the entrance to the TSPs where flashing is proposed to cause localized boiling and precipitation onto the TSP [67, 68].

Consolidation of the deposit manifests itself by a reduction in the rate of particle removal from the deposit, as shown in Figure 6. The graphs in the Figure show Fe-59 radiotracing data for the deposition and removal of magnetite particles at a heat-transfer surface under flow-boiling conditions with the pH controlled by morpholine (top) and by dimethylamine (bottom) [63]. Clearly, the amine used for pH control has a significant effect on the rate of removal of particles from the surface. This phenomenon has been interpreted as evidence for the effect of the amine on the rate of deposit consolidation [69], as discussed further in Section 3.2.2.

3.2 Modeling Particulate Fouling

3.2.1 Fouling of an Un-heated Surface

A simple model of particulate fouling of an un-heated surface can be constructed by taking account of steps 2, 3, and 4 and the mechanisms discussed in Sections 3.1.2, 3.1.3 and 3.1.4. Starting with:

$$\dot{m}_s(t) = \dot{m}_d(t) - \dot{m}_r(t) \quad (18)$$

and substituting Equation (6) and Equation (16) for $m_d(t)$ and $m_r(t)$, respectively, one can solve to obtain:

$$m_s(t) = (K_d \rho_f/\lambda_r) (C_b - C_s) (1 - \exp (-\lambda_r t)) \quad (19)$$

Models of particulate fouling of the form shown in Equation (19) are called Kern-Seaton models after the investigators who first suggested modelling the rate of fouling as the difference between a rate of particle deposition and a rate of

TABLE 1: Recommended Fouling Models for Four Different Scenarios; with and without Removal, and Before and After Monolayer Coverage

	Particle Removal $(d_p U^*/\nu) > 1$; $\lambda_r > 0$	**No Particle Removal** $(d_p U^*/\nu) < 1$; $\lambda_r \sim 0$
$m_s < m_{monolayer}$	$m_s(t) = (K_d \rho_f/\lambda_r)(C_b - C_s)(1 - \exp(-\lambda_r t))$	$m_s(t) = \rho_f K_d (C_b - C_s) t$
$m_s > m_{monolayer}$	$m_s(t) = (\rho_f K_a C_b - \lambda_r m_{monolayer}) t$ for pH ≠ IEP of the particle. Otherwise, $m_s(t) = (\rho_f K_t C_b - \lambda_r m_{monolayer}) t$	$m_s(t) = \rho_f K_a C_b t$ for pH ≠ IEP of the particle. Otherwise, $m_s(t) = \rho_f K_t C_b t$

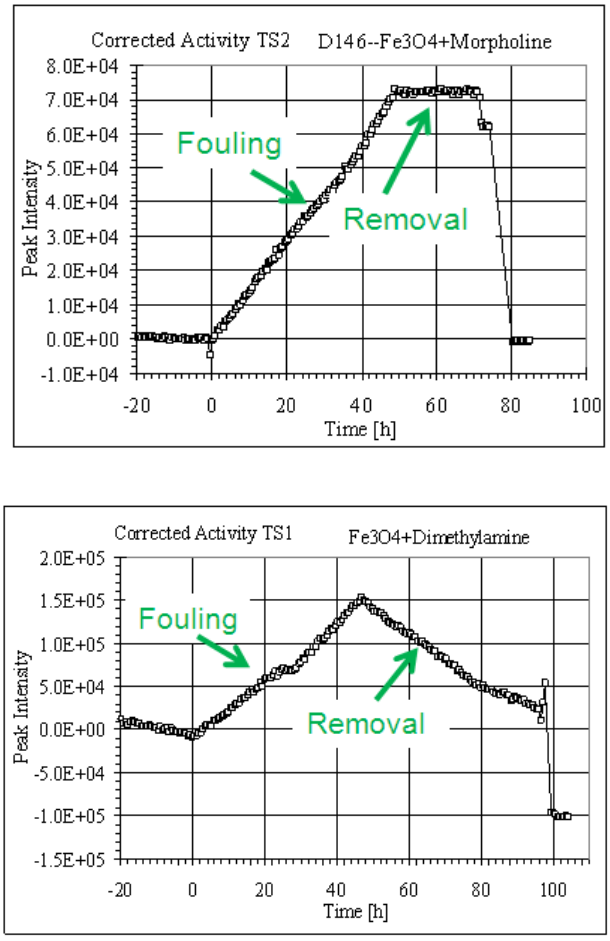

FIGURE 6: Illustration of the effect of consolidation on the rate of particle removal from a heat-transfer surface; top: high consolidation rate;bottom: low consolidation rate [63].

particle removal, with the removal rate being proportional to the deposit mass [70]. Equation (19) shows that the deposit mass will initially build up on the wall at a rate equal to $\rho_f K_d (C_b - C_s)$. Eventually, the rate of accumulation will be reduced as the rate of particle removal increases in proportion to the deposit mass until the deposit mass reaches the asymptotic value of $\rho_f K_d (C_b - C_s)/\lambda_r$. This, of course, presumes that the particles are large enough to be removed from the wall by the hydrodynamic forces, i.e., $(d_p U^*/\nu) > 1$, as suggested in Section 3.1.4. As noted in Section 3.1.4, it is not realistic to assume that the rate-of-deposit removal is proportional to the deposited mass once a monolayer coverage of particles on the wall has been exceeded. Thus, a more realistic approach to modeling would be to use Equation (18) for deposit loading less than one monolayer coverage, and for $m_s(t) > m_{monolayer,}$ use:

$$m_s(t) = (\rho_f K_d (C_b - C_s) - \lambda_r m_{monolayer}) t \qquad (20)$$

For $(d_p U^*/r) < 1$, the rate of removal is negligibly small, and so the rate of fouling of the wall can be approximated by Equation (20) with $\lambda r \approx 0$.

Note that for deposition under transport control, where the particle and the wall are of opposite sign of charge, once there is a monolayer of particles on the wall it is inevitable that an in-coming particle will now encounter a surface of the same sign of charge as the particle itself. Thus, one would expect that deposition under transport control would transition to control by attachment as deposit on the wall builds up to a monolayer, provided that the particle has a non-zero charge. For deposition of particles onto a wall of like sign of charge, deposition is already under attachment control, and so one would not expect to see a significant change in deposition rate once a monolayer of coverage has been attained. For deposition at pH = IEP of the particle, the deposition rate will always be under transport control. Models of particulate fouling for four different scenarios, with and without removal and before and after monolayer coverage, are listed in Table 1.

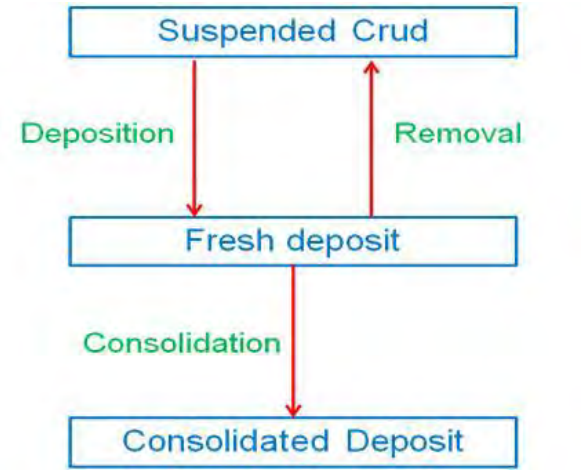

FIGURE 7: Model of particulate fouling onto a heated surface illustrating the rate processes of deposition, removal, and consolidation.

3.2.2 Fouling of a Heated Surface

A model of the fouling of a heated surface must take account of the effect of the temperature gradient on the rate of transport of the particle from the bulk fluid to the heated surface, as well as the effect of deposit aging, or consolidation, as discussed in Section 3.1.5.

Particles in a temperature gradient will tend to move from the hotter region to the cooler region of the fluid. This phenomenon can be understood as being the result of molecules in the hotter fluid having higher kinetic energy and, therefore, imparting more momentum when they collide with the particle than do molecules from the cooler region of the fluid. The migration of particles away from a heated surface and, by the same phenomenon, towards a cooled surface is called thermophoresis. The thermophoretic velocity of a particle down a temperature gradient has been calculated by McNab and Meisen [71]:

$$K_{th} = 0.26\, h\, \nu\, \Delta T/((2\,\kappa_f + \kappa_p)\, T_b)) \qquad (21)$$

The effect of the thermophoretic velocity on the overall rate of particle transport to a heated surface has been demonstrated by Turner and Smith [72] for the fouling of a heated surface of Alloy 600 by sub-micron particles of magnetite.

A model that takes account of the effect of deposit consolidation on the rate of deposit accumulation on a heated surface has been developed by Turner and Klimas [63], and is shown conceptually in Figure 7. Once a particle has been deposited onto the surface, it is subject simultaneously to the processes of removal and consolidation. Only the particles that have not yet been consolidated are subject to removal. Once they have become consolidated, they can no longer be removed.[11] Mathematically, this is expressed by two equations: one which calculates the time rate of change of the total deposit mass and the other that calculates the time rate of change of the removable (unconsolidated) portion of the deposit mass. Solving these two simultaneous equations and integrating, one obtains [63]:

$$m(t) = (\rho_f K_d C_b/\lambda)\cdot(t\lambda_c + (\lambda_r/\lambda)\cdot(1 - \exp(-\lambda\cdot t)) \qquad (22)$$

where $\lambda = \lambda_r + \lambda_c$

The model predicts the accumulation of a bi-layered deposit that consists of a dense (consolidated) inner layer overlain by a porous, un-consolidated outer layer. The predicted fouling kinetics can be linear, asymptotic or falling-rate, as illustrated in Figure 8, depending on the relative magnitudes of the rate constants for deposition, removal and consolidation.

A method for determining the ratios λ_r/λ and λ_c/λ in Equation (22) from plots of fouling and removal data (see, for example, Figure 6) is described in Reference [63]. Because consolidation affects the rate of fouling itself, however, the magnitudes of the individual parameters λ_r and λ_c in Equation (22) could not be determined. From investigations of particulate fouling under sub-cooled and saturated flow-boiling in a loop operating at < 100 °C, Lister and Cussac proposed an expression for the consolidation rate constant, λ_c [73]:

$$\lambda_c \propto (1 - m_{labile}) \qquad (23)$$

where,

$$m_{labile} \propto A_{site}\cdot N_{active}/(q/L) \qquad (24)$$

The labile portion of the deposit defined in Equation (24) is equivalent to the fresh, unconsolidated deposit identified in Figure 7.

3.3 Experimental Investigations

3.3.1 Forced Convective Turbulent Flow: Deposition, Attachment and Removal

Investigations of particulate fouling in an aqueous, turbulent flow are based on several different methods for determining the mass of material that has accumulated on the wall of the test section as a function of time, including: thermal resistance [74, 75], absorption of X-rays [76, 77, 78, 79, 80] and radiotracer methods using neutron-activated particles [72, 81, 82, 83, 85]. Derivation of the deposit

[11] The model does not take account of spalling of larger pieces of consolidated deposit, but this would be an obvious extension of the model.

mass from a measurement of either thermal resistance or x-ray absorption is subject to uncertainty because the relationship between deposit mass and either of these quantities depends on the deposit density, which is generally not well known under the experimental conditions and can even change with time as the result of consolidation (see the discussion in Section 3.1.5).

Of the methods listed above, only radiotracing using neutron-activated particles that emit high-energy gamma rays provides a direct measure of the deposit mass independent of the deposit density. Experimental investigations of particulate fouling in a turbulent flow are inherently difficult because of the challenges associated with maintaining constant experimental conditions for a prolonged period of time, especially maintaining a constant concentration of particulates in the turbulent flow. In this respect, it is better to do experiments in small loops rather than large ones, and to use small, stirred tanks to maintain constant particle concentration rather than large tanks where particle agglomeration and settling can result in a major uncertainty regarding the concentration of suspended particulate during the test.

Investigations of magnetite particulate fouling from an aqueous turbulent flow onto aluminum tubes were conducted in a test loop at Harwell by Gudmundsson [76] and by Newson [77]. The suspension of particulates was maintained in a tank of volume 2,300 litres, which presented challenges with respect to the ability to maintain a constant concentration of suspended particles throughout each test. The deposit mass was calculated from measurements of the absorption of x-rays as a function of time as deposit built on the test section. The deposition/time curves were jagged, suggesting intermittent removal of parts of the deposit from the wall of the test section during the runs. Based on runs at two different flow velocities, it was deduced that the rate of particle deposition varied inversely with the fluid velocity [76]. An additional seven runs were subsequently performed on the same loop to do a more detailed investigation of the velocity dependence of the deposition rate. The runs were conducted at 40 ˚C using a suspension of magnetite particles of nominal particle size 2 μm. The results were fitted using a Kern-Seaton fouling asymptotic model. Based on these latter results, it was suggested that the deposition velocity increased with fluid velocity to the power 2.2 [77]. Neither of these two investigations resulted in a particle deposition velocity that is consistent with diffusion control, which is what would be expected for 2 μm particles under the test conditions.

The investigation of particulate fouling from flowing suspensions of magnetite in turbulent flow was continued by Newson *et al*. [78, 79] and by Hussain *et al.* [80] in a loop for which the suspension of particles was maintained in a stirred, 45 litre vessel. The runs were conducted at pH 6.8, and the deposit mass on the test section was determined by x-ray absorption, as before. It was later learned that spurious errors in measurement were due in part to the difficulty in maintaining constant strength of the x-ray beam. An analysis of the particles used for this investigation showed particle sizes ranging from 1 to 5 μm, with an average size of 1.5 μm. The data were analysed using an asymptotic Kern-Seaton model. Analysis showed that the initial deposition rate varied as fluid velocity to the exponent 0.73, which is in good agreement with a diffusion mechanism for particle transport. The authors also showed that correlations developed for particle transport in aerosol systems predict that interial transport should be the dominant mechanism for particle deposition under the test conditions. It appears, however, that the correlations developed for interial transport for aerosols over-predict the magnitude of intertial transport by several orders of magnitude when applied to aqueous systems [44, 52]. The asymptotic deposit mass determined from the fit of the Kern Seaton model to the fouling data showed a dependence on U raised to the exponent -0.66, which implies that a particle-removal mechanism could be limiting the build-up of deposit.[12]

The earliest investigation of particle deposition in an aqueous, turbulent flow using radiotracer techniques was made by Thomas and Grigull [81]. Using particles of magnetite with a mean size of 0.06 μm and radiotraced with Cr-51, which decays with the emission of a gamma ray, they found that the particle fouling rate in high-temperature neutral water increased linearly with the Reynold's number under single-phase isothermal conditions, which is consistent with particle transport from the bulk to the wall by a diffusion mechanism. Each test lasted only a few hours, and the deposition rate was observed to decrease about five-fold during this period of time. Thomas and Grigull observed that this behaviour is consistent with a falling "sticking probability".

Newson *et al.* [82] conducted an extensive investigation of fouling by 0.2 μm hematite particles suspended in a turbulent flow onto the surface of a 316 stainless-steel (SS) tube. The tests were conducted in a simple loop with a suspension of hematite particles maintained in a 50 litre vessel. There is no indication as to whether the suspension was stirred during each test. Runs were conducted as a function of pH, fluid temperature and fluid velocity using hematite particles that had been neutron-activated to produce Fe-59, an unstable isotope of Fe that decays with the emission of a gamma ray. The deposit mass on the test section was measured as a function of time using a sodium-iodide gamma ray detector. For a series of runs done at pH 6.8, the initial rates of

[12]The values of the exponent for the dependence of the deposition velocity and asymptotic deposit mass on U quoted in the text are from References [78] and [79]. The magnitudes, but not the signs, of the exponents are reversed in Reference [80] for the same body of work.

particle deposition increased with fluid velocity in a manner consistent with particle transport to the wall by a diffusion mechanism. The plot of deposition velocity versus pH went through a maximum at pH 6.2 [83]. No measurements were made of the IEPs of either the hematite particles or the 316 SS surface used in this investigation, and the effect of pH on the deposition velocity was interpreted in terms of a pH-dependent "sticking probability". The authors noted the similarity between their results and the results of Kuo and Matijevic, who observed that the mobility of hematite particles through a packed bed of stainless steel went through a maximum at a pH of 6.8 [84]. Measurements were also made of the particle-removal rate by switching from a suspension of active hematite particles to inactive particles, and measuring the deposit activity as a function of time. The authors reported no measurable removal of particles from the wall up to a Reynold's number of 140,000. Some of the experiments, however, indicated a falling deposition rate, which the investigators interpreted in terms of gradually decreasing "sticking probability". Even though many of the runs did not reach an asymptote, a Kern-Seaton model was fitted to the data and a relationship was established between the fitted asymptotic deposit mass and the fluid velocity.

A detailed investigation of fouling by magnetite particles suspended in a turbulent flow was conducted as a function of pH, fluid temperature, fluid velocity and temperature gradient [72, 85]. The neutron-activated particles of magnetite were nearly-monosized with a mean particle size of 0.26 μm, and the deposit mass was determined during each run as a function of time using a high-efficiency gamma ray detector. For each experiment, after establishing a fouling rate the suspension of active particles was switched out of the circuit and replaced with a solution of deionized water at the same pH as the suspension to measure the rate of particle removal from the wall. The fouling rate was observed to be a strong function of pH, going through a maximum near a pH of 7.5 and 7.1 for deposition onto surfaces of Alloy 800 [85] and Alloy 600 [72], respectively. The effect of pH was interpreted in terms of the relative surface potentials of the magnetite particles and the substrates, with the surfaces being presumably oppositely charged in the pH-range of 6 to 8 (where the deposition rate goes through a maximum), and similarly charged for pH outside of this range. The measured rate of particle removal during the "release" phase of each test was very small, from which a removal rate constant, $\lambda_{r,}$ was estimated to be $4 \bullet 10^{-7}$ s^{-1}. The deposition velocity at pH 7 showed an approximately linear dependence on fluid velocity raised to the power 0.5 for U* up to 0.15 m/s, whereupon the deposition velocity showed an abrupt decrease for U* > 0.15. A similar result was observed for fouling of a sand/water mixture where an abrupt decrease in deposition rate was observed for U* > 0.12 m/s [74]. This latter behaviour is interpreted as evidence for the onset of significant particle removal for a particle size greater than a critical value for a given fluid velocity [72] (see discussion of particle-removal criteria in Section 3.1.4).

Burrill conducted an investigation of the deposition of magnetite particles onto zirconium alloy and nickel surfaces at temperatures of 25 and 90 °C [86]. Fluid velocities between 5 and 100 m/s were achieved by forcing a suspension of magnetite particles to pass through small tubes under a high, applied pressure of air. The tests were very short, lasting only from 0.3 to 6 seconds. Deposits were removed after each test by acid dissolution, and this information was used along with the test duration to calculate a deposition velocity for each test. For tests at neutral pH and Re between ~ 20,000 and ~ 50,000, the fouling rate on the nickel tube increased as Re6, decreasing to a 0.8 power dependence for Re > 100,000. Burrill interpreted this behaviour as evidence for inertial deposition at lower Re, changing to a diffusion-controlled mechanism at the higher Re. In additional tests, the deposition rate constant was shown to increase with increasing concentration and with increasing temperature. Burrill also measured the pH dependence

TABLE 2: Comparisons of Key Parameters Related to Particle Transport and Removal Derived from Various Investigations of Particulate Fouling

Reference	d_p (μm)	t_p^+	U* (m/s)	(d_pU^*/ν)	Initial Fouling Rate $\propto U^{\alpha}$
[76]	~ 2	-	-	-	$\alpha = -1$
[77]	~ 2	$1.5 \cdot 10^{-3}$ to $1.5 \cdot 10^{-2}$	0.025 to 0.073	0.08 to 0.24	$\alpha = 2.3$
[78] [80]	~ 1.5	$2 \cdot 10^{-4}$ to 0.11	0.062 to 0.16	0.05 to 0.55	$\alpha = 0.5$ to 1.0
[84]	~ 0.06	$1.3 \cdot 10^{-4}$ to $6.4 \cdot 10^{-4}$	0.055 to 0.086	0.03 to 0.04	$\alpha \sim 1$
[85]	~ 0.2	$1.2 \cdot 10^{-4}$ to $1.9 \cdot 10^{-3}$	0.072 to 0.17	0.02 to 0.08	$\alpha \sim 1$
[86]	~ 0.25	$1.1 \cdot 10^{-4}$ to $6.4 \cdot 10^{-4}$	0.072 to 0.168	0.02 to 0.05	$\alpha \sim 0.5$
[87]	~ 1	0.03 to 0.16 0.28 to 5.6	0.29 to 0.67 0.89 to 4.0	0.32 to 0.78 0.98 to 4.4	$\alpha \sim 6$ $\alpha \sim 1$

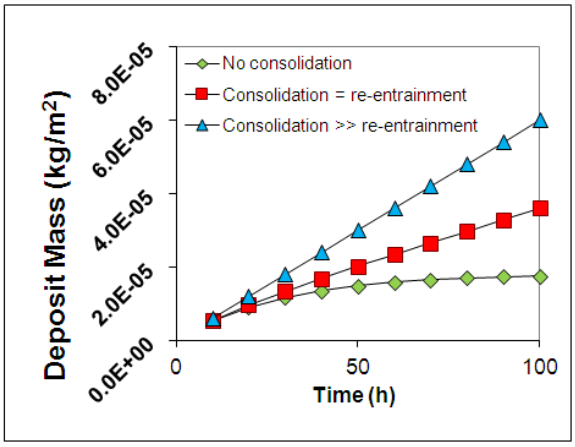

FIGURE 8: Particulate fouling kinetics predicted by (22) for three different cases: i) no consolidation, ii) consolidation = removal, and iii) consolidation >> Removal [63].

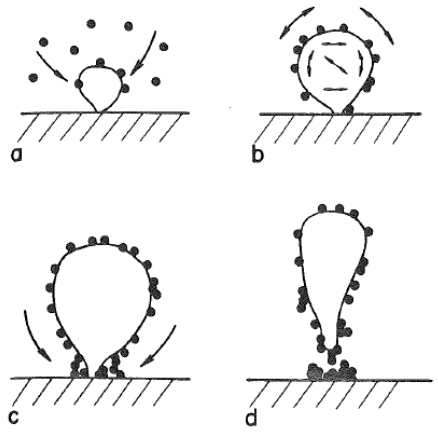

FIGURE 9: Illustration of the four stages leading to accumulation of hydrophobic particles at bubble nucleation sites on a surface under boiling heat-transfer; a) collection, b) surface migration, c) accumulation, and d) bubble departure [80].

of deposition onto a tube of Zircaloy-4 and found that the deposition rate was highest at pH 4 and lowest at pH 10, with an intermediate deposition rate constant at pH 7.

A comparison of the key parameters related to particle deposition and removal for the investigations discussed in Section 3.3.1 is listed in Table 2. For those studies that included deposition under both transport-limited and attachment-limited conditions, the U-dependence of the initial fouling rate listed in Table 2 is from the subset of tests that were done under transport limited conditions, i.e., for the pH-range for which the deposition rate goes through a broad maximum with respect to pH. A comparison of the results from these investigations leads to the following conclusions:

1. The rate of removal of deposited particles from a wall in a turbulent flow is negligible when $d_p U^*/\nu <\sim 1$, i.e., the particle size is less than ~20% of the thickness of the laminar sub-layer.
2. The deposition rate under transport-limited conditions is well described by a diffusion-limited process for $t_p^+ \leq 0.1$.
3. Correlations for inertial transport, which show good agreement with particle transport behaviour in aerosol systems, over-estimate particle transport rates in aqueous systems by several orders of magnitude. The results from Reference [86] not withstanding, inertial transport may not be applicable to particle transport in aqueous systems.

3.3.2 Flow-boiling

3.3.2.1 Impact of Boiling on Rate of Particulate Fouling

The impact of boiling on the fouling of heat-transfer surfaces was of particular concern to the nuclear industry in the early days of the development of commercial nuclear power reactors. Some early studies suggested that the fouling rate under flow-boiling conditions was proportional to the product of the concentration of corrosion product with the square of the heat flux [87, 88, 89]. These investigations did not elucidate the relative contributions from fouling by soluble versus particulate corrosion products; therefore, they presented their results in terms of the total iron concentration.

Thomas and Grigull investigated fouling under flow-boiling conditions in a series of short (usually up to four hours) tests in a loop using magnetite particles radiotraced with Cr-51. They found that the particulate fouling rate increased with the onset of sub-cooled nucleate boiling, and that the fouling rate continued to increase as the degree of sub-cooling decreased [81]. They also showed that the fouling rate increased linearly with heat flux, which suggests that the enhancement of particulate fouling may be directly related to the rate of bubble nucleation on the heat-transfer surface. Thomas and Grigull, however, attributed the increase to a higher fluid turbulence and mass transport to the surface with the onset of boiling. Nicholson and Sarbutt conducted loop fouling tests under BWR conditions, and observed higher fouling rates of hematite particles on surfaces in boiling heat-transfer compared to heat-transfer without boiling [90]. Like Thomas and Grigull, they also observed an increase in deposition rate with decreased sub cooling. Iwahori *et al.* studied the effect of boiling on the fouling of heated wires of Zircaloy-2 and stainless steel by particles of hematite at 100 °C [91]. They, too, observed an enhancement of the rate of particulate fouling in the presence of boiling,

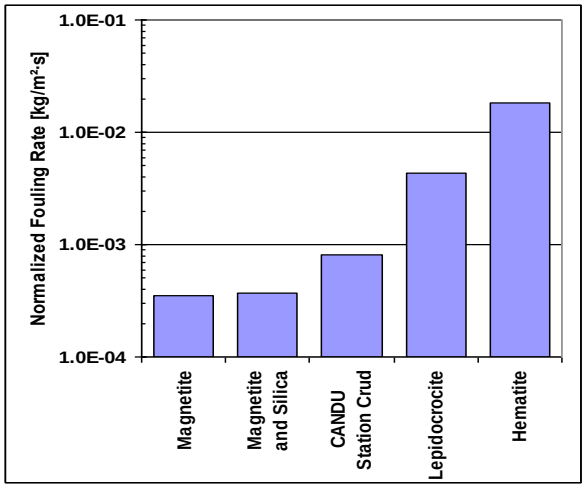

FIGURE 10: Measured particulate fouling rates for different corrosion products under flow-boiling conditions at a $pH_{T=270°C}$ of 6.2 adjusted using morpholine [63].

and observed that the deposits initially formed as rings around bubble nucleation sites. Significantly, they also showed that deposit of similar morphology was formed on un-heated surfaces around bubbles that were produced at the surface by a flow of air bubbles introduced from a capillary. These observations led Iwahori *et al*. to postulate that enhanced deposition under boiling heat-transfer was the result of metal oxide particles collecting on the surface of bubbles growing at the surface of the substrate. It was proposed that the particles move on the surface of the bubble and eventually collect in rings at the base of the bubble as the bubble detached from the surface. To support this hypothesis, the authors showed photographs of particles that had collected on the surfaces of bubbles that formed on the heat-transfer surface.

Figure 9, taken from the paper by Iwahori *et al.*, illustrates the various stages of the particle-bubble interaction that are proposed to lead to the accumulation of particles at the bubble nucleation site [91]. In the first step (a), particles collect on the surface of a growing bubble. The collected particles continue to move around the surface of the bubble as it grows (b). Particles also migrate towards the heat-transfer surface (c). Finally, the bubble grows large enough to depart from the surface (d), carrying some particles with it back to the bulk and leaving behind a ring of deposited particles on the surface.

Asakura *et al.* demonstrated a linear effect of particle concentration and heat flux on the rates of fouling by particles of hematite onto the heated surface of Zircaloy 2 under flow-boiling conditions at a pressure of 1 atm. [92]. Similar results were later obtained in a natural circulation loop operating at a pressure of 10 atm. [93]. Asakura *et al.* also observed that the deposit formed at sites of bubble nucleation, and that the deposit morphology was circular. They invoked the theory of microlayer evaporation to develop a model of boiling-enhanced deposition to account for the observed deposit morphology and predict the boiling-enhanced deposition rate as a function of thermal-hydraulic conditions. More recently, Bassett *et al*. [94], Carpentier *et al.* [95], and Arbeau *et al*. [96] have all investigated particulate fouling of a heated surface in sub-cooled flow-boiling at 90 ˚C, and found linear relationships between the fouling rate and both heat flux and the concentration of particles in suspension.

3.3.2.2 Investigations of Particle-bubble Interactions

To further our understanding of the mechanism of boiling-enhanced fouling of heat-transfer surfaces, a number of investigations have been conducted at atmospheric pressure where high-speed photography can be used to interrogate the process of bubble nucleation and growth, and the interaction of the bubbles with particles in suspension.

For example, Wen and Melendres investigated fouling of a stainless-steel surface by hematite particles under nucleate boiling conditions at 100 ˚C [97]. The experiments were conducted in a glass cell with a heated steel disk at the bottom. The temperatures of the disk and suspension of particles were controlled separately to control the rate of bubble nucleation and bubble residence time on the surface. Formation and growth of individual bubbles was observed in real time, and the bubble size and residence time were correlated with the amount of deposit formed. Their investigation found that particles deposited primarily at the boundary of the gas/liquid/solid interface, consistent with the ring pattern of deposit reported by other investigators. The amount of deposit was correlated with the bubble size and its residence time on the heat-transfer surface. The authors conclude that their observations are not consistent with the microlayer evaporation theory, and that bubble-particle interactions play a dominant role in determining the boiling-enhanced fouling rate.

Basset *et al.* studied fouling by magnetite particles of Alloy-800 heated surfaces under sub-cooled nucleate boiling conditions in a loop operating at 90 ˚C [94]. The magnetite particles were radiotraced with Fe-59 so that fouling rates could be measured continuously using a gamma ray detector. A video camera was used to record bubble nucleation and growth as well as the particle-bubble interactions in sub-cooled nucleate boiling. Basset *et al*. proposed that when the fluid is highly sub-cooled and the bubble lifetime is relatively long, particle-bubble interactions dominate the deposition process resulting in ring-shaped deposits. As the

degree of sub-cooling decreases, bubble lifetimes decrease and microlayer evaporation is the dominant process, giving rise to disk-shaped deposits. This hypothesis may offer a means to reconcile the apparently divergent conclusions of Wen and Melandres [97] (who investigated bubble formation in a non-flowing system) with those of Asakura *et al*. [92, 93] regarding the relative importance of microlayer evaporation and particle-bubble interactions with respect to the mechanism of particle deposition in boiling water.

Lister and Cussac have proposed a model of particle fouling under sub-cooled and saturated flow-boiling conditions based on continuing studies of particle deposition at the University of New Brunswick [73]. The model is based on microlayer evaporation, and incorporates observations made of the process of bubble nucleation and growth and particle-bubble interactions observed using high-speed video photography. The model considers both deposition and removal at a single bubble nucleation site. In the early stages of deposit formation when the surface coverage is sparse, the deposition rate is governed by microlayer evaporation. As deposit accumulates on the surface, an additional deposition mechanism occurs whereby suspended particles are filtered by the deposit as liquid is drawn towards the heat-transfer surface and boiled. Turbulence created by collapsing and detaching particles affects particle removal. The model predictions agree well with the experimental data presented.

3.3.2.3 Effect of Water Chemistry: pH, Alternative Amines and Dispersants

The investigations described in the previous sections highlight the important role of surface interactions in determining the overall rate of particulate fouling under boiling heat-transfer conditions. Attachment of particles to a growing bubble and the migration of particles on the surface of the bubble during bubble growth are expected to be influenced by factors such as the surface tension of the steam/water interface, surface tension gradients across this interface, and the relative surface charges of the steam/water and the particle. Water-treatment chemicals added to control pH, for example, or to inhibit fouling, may influence the fouling rate through their effect on the surface tension, the surface tension gradient or surface potentials. All three of these factors influence the dynamics of the particle-bubble interaction, and therefore could play a dominant role in determining the rate of particulate-fouling under flow-boiling conditions. In this section, several investigations that illustrate the influence of water chemistry on the rate of particulate fouling under flow-boiling conditions are reviewed.

Iwahori *et al*. [91] investigated the effect of pH on fouling of heated wires by particles of hematite under both flowing and non-flowing conditions. Both sets of tests showed a pH-dependence of the fouling rate, although the pH dependence observed for the non-flowing tests was not the same as observed in the tests under flowing conditions. Under flowing conditions, the fouling rate was highest at pH 6, and decreased as the pH was either raised or lowered from this value. Under non-flowing conditions, the fouling rate was lowest in the range pH 8 to 9, and went through a maximum near pH 4 and near pH 11.5. The IEP of hematite at ambient temperature is reported to be at pH 9.1. The stability of colloidal suspensions is known to be at a minimum at the IEP [55], so it is possible that agglomeration and settling may have reduced the fouling rate in the tests under non-flowing conditions at pH values in the vicinity of the IEP.

Both Bassett *et al*. [94] and Arbeau *et al*. [96] measured the pH-dependence of the fouling rate of a heated surface of Alloy-800 by magnetite particles under sub-cooled flow-boiling conditions. Bassett *et al.* reported a maximum in the fouling rate centred at about pH 8, while Arbeau reported a similar dependence with a maximum at about pH 7.5. These results are in good agreement with measurements by Turner *et al*., who reported that the fouling rate of magnetite particles onto the surface of Alloy-800 under single phase forced convection was a strong function of pH, and went through a maximum at approximately pH 7.5 [85]. All three sets of investigators concluded that the pH-dependence of the fouling rate was related to the pH-dependences of the surface potentials on both magnetite and Alloy-800, and that the range of pH for which the fouling rate went through a broad maximum corresponds to the pH range where the respective surfaces are oppositely charged.

The effect of surface chemistry on the rate of particulate fouling was extensively investigated in a collaborative program by Atomic Energy of Canada Limited and the Electric Power Research Institute [63, 69, 98, 99, 100, 101, 102]. All tests were conducted in the B250 H3 high-temperature water chemistry loop at Chalk River Laboratories (CRL). The tests were conducted under flow-boiling conditions at a temperature of 270 ˚C and steam qualities ranging from -0.3 (sub-cooled) to > +0.50. The test program investigated the effect of the type of corrosion product (magnetite, hematite, lepidocrocite) and water-treatment chemical (various volatile amines, including ammonia, morpholine, ethanolamine, dimethylamine, and others) on the rate of particulate fouling as a function of steam quality. The concentrations of the amines used were adjusted so that all the tests were done at the same high-temperature pH (pH_T) of 6.2, calculated at zero steam quality.[13]

The tests demonstrated a strong influence of surface chemistry on the fouling rate. For example, it was shown

[13] Because the amines are volatile, one would expect a change in the concentration of amine and, therefore, pH_T with increasing steam quality. The deposition rates measured, however, were independent of steam quality in these tests for steam quality between 0 and 0.25. Therefore, the effect of any change in pH_T with increasing steam quality is not being reflected in the deposition rates measured in these experiments.

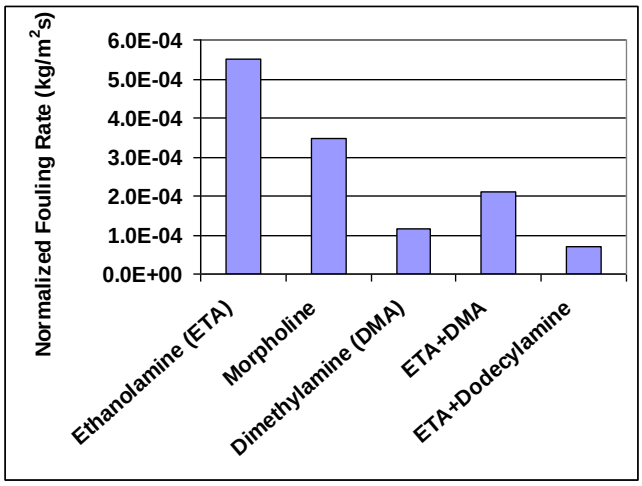

FIGURE 11: Influence of amine used for pH control on the fouling rate of magnetite particles under flow-boiling conditions [63].

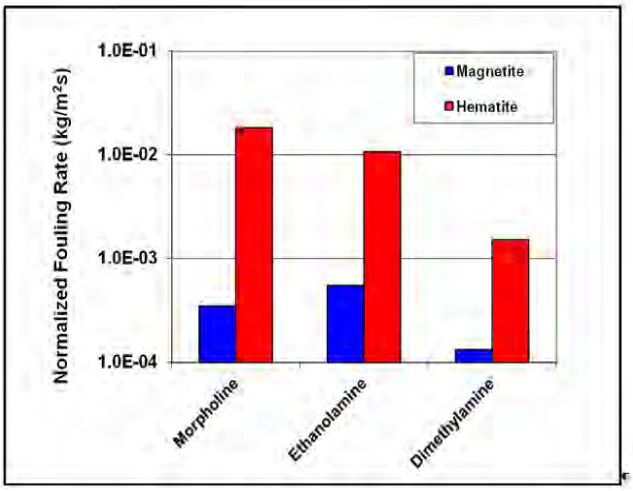

FIGURE 12: Influence of amine used for pH control on the fouling rate of particles of hematite and magnetite under flow-boiling conditions [100].

that the fouling rate by hematite particles is significantly higher than that of magnetite particles, with the fouling rate of lepidocrocite particles coming in between, as illustrated in Figure 10 [63].

The fouling rate of hematite relative to magnetite was explained in terms of the difference in the IEPs of the two oxides at 270 ˚C, i.e., magnetite particles are predicted to be negatively charged under the test conditions (i.e., pH_T > IEP at 270 ˚C), while the hematite particles are predicted to be positively charged (i.e., pH_T < IEP at 270 ˚C) [103]. The IEPs of Fe-Cr-Ni alloys have not been measured at high temperatures but based on measurements of the IEP of stainless steel at room temperature, one would expect the surface of Alloy 800 to be negatively charged under the test conditions, which is consistent with the relative fouling rates observed for hematite and magnetite particles. These results may be interpreted as illustrating the effect of surface potential on the rate of particle accumulation on a heat-transfer surface under flow-boiling conditions as a result of deposition from the evaporating microlayer at the bubble nucleation site.

The AECL EPRI collaborative investigation also showed evidence for a strong effect of the amine used for pH control on the overall fouling rate, as illustrated in Figures 11 and 12 for fouling by particles of magnetite and hematite, respectively, under flow-boiling conditions.

The origin of the effect of amines on the rate of particulate fouling under flow-boiling conditions was not fully elucidated during the course of these investigations. Several avenues of inquiry were followed, including investigations of the surface adsorption, atomic force microsocopy and surface-tension measurements to try to understand the mechanism by which the amine was affecting the fouling rate. Ultimately, however, no single phenomenon was able to account for the observed results.

The effect of using dodecylamine (DDA) in combination with ETA for pH control is particularly interesting because this combination resulted in the lowest fouling rates measured [104]. DDA is known as a filming amine, a group of aliphatic amines that have been added to the steam cycles of fossil-fired boilers to mitigate corrosion. There has recently been a renewed interest in the use of filming amines to mitigate fouling of nuclear SGs. If the results shown in Figure 11 are any indication, the use of filming amines to mitigate SG fouling may be well worth pursing.

Dispersants are a class of surface-active agent that have been used extensively to mitigate fouling of fossil-fired boilers in the utility and process industries. Investigations of the effect of chemical dispersants on particulate fouling under

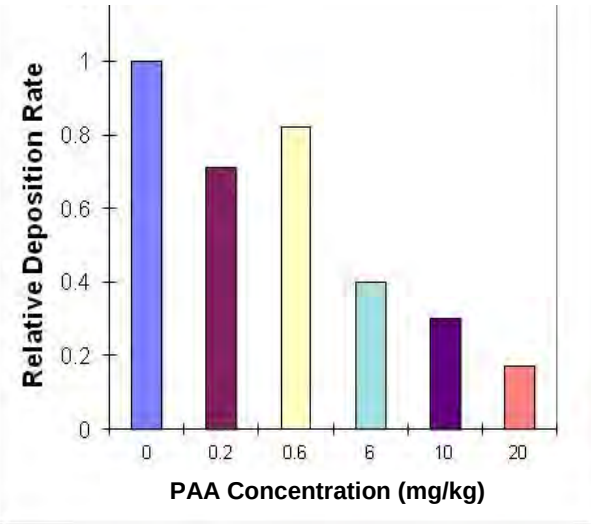

FIGURE 13: Effect of the concentration of a low molecular weight polyacrylic acid on the rate of fouling by magnetite under flow-boiling conditions at a room temperature pH between 9.2 and 10.1 adjusted with morpholine.

flow-boiling conditions were conducted in the B250 H3 loop at CRL [105, 106]. These investigations identified several potential candidates that appeared to be suitable for use in a nuclear SG, including low molecular weight polyacrylic acid (PAA). The effectiveness of the concentration of PAA on the fouling rate under flow-boiling conditions is illustrated in Figure 13.

Interestingly enough, dispersants that were effective at mitigating fouling under flow-boiling conditions were often not effective when tested under single-phase forced convection. This implies that the effectiveness of dispersants is related to the particle-bubble interaction rather than through a surface repulsion mechanism.

3.3.3 Fouling of the Tube-support Structure

As discussed in Section 2.3, fouling of the tube-support structure has affected all nuclear SG designs that use either the trefoil or the quatrefoil TSP design. TSP fouling is characterized by the accumulation of very hard deposit at the inlet to the flow passages on the TSP itself. Deposit grows not from the heat-transfer surface, but from the surface of the TSP. As the deposit grows, the flow passage is increasingly blocked, leading to serious operational problems and materials degradation that challenge safe, economic reliable operation of the SGs.

With the trefoil and quatrefoil design, there is an abrupt reduction in the cross-sectional area to flow as the two-phase mixture on the secondary side of the SG enters the flow holes of the TSP. This abrupt reduction in flow cross-sectional area results in separation of the fluid boundary layer from the surface of the TSP, which causes the main flow to contract through a minimum cross-sectional area called the *vena contracta*. Associated with the *vena contracta* is a corresponding local maximum in fluid velocity, a local minimum in pressure and a local maximum in turbulence intensity. These localized phenomena at the entrance to the TSP have been verified by numerical modelling [107] and by measurements under single phase and two-phase flow conditions [68, 108]. The various phenomena that may contribute to the accumulation of deposit on the TSP surface at the entrance to the flow passages are identified in Figure 14 [68].

The separation of the boundary layer from the surface of the TSP at the entrance gives rise to three phenomena that act to promote the accumulation of deposit:

1. High-turbulence intensity and mass transfer coefficient increase the rate of particle transport from the bulk fluid to the wall,
2. Particles transported into the low-velocity circulation zone of the *vena contracta* will have little tendency to be removed because the hydrodynamic forces in this region will be very low, and,
3. Precipitation of dissolved iron caused by flashing of the two-phase mixture at the *vena contracta* will contribute to deposit consolidation at this location.

A detailed model based on the various hydrodynamic forces acting on a particle together with the phenomena described above has been developed to account for the fouling of TSPs in nuclear SGs [31, 68]. More recently, Prusek *et al*. developed a model of TSP fouling based on the studies of Rummens *et al.* [68] and used it in conjunction with a

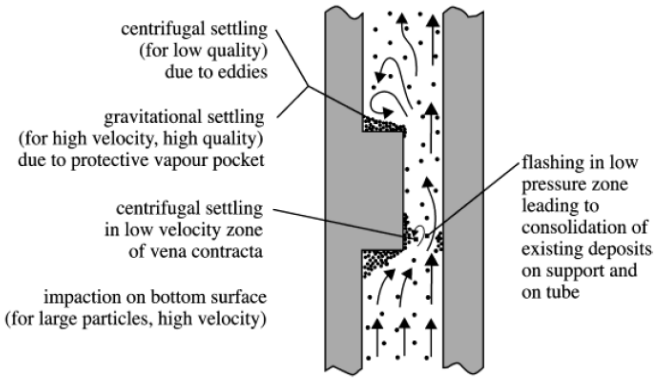

FIGURE 14: Illustration of potential contributing factors to fouling of orifices under flow-boiling conditions [68].

thermal-hydraulics code developed by EdF to compare to TSP blockage of quatrefoils in SGs in the French fleet [109]. The model takes account of changes in the fluid hydraulics as blockage of the TSPs progresses.

An alternative mechanism for TSP fouling has been proposed based on work by Beck *et al*. [110] and the investigations of the blockage of flow orifices used for boilers of Advanced Gas Reactors [111, 112]. The mechanism is based on the effect of the streaming potential that develops when a fluid flows past a charged surface. The streaming potential is one of four electrokinetic phenomena that are associated with the relative flow of a fluid with respect to a charged surface. These phenomena are well-described in the literature [113], and will not be discussed in detail here. Thus, for aqueous systems, uniform flow with respect to a pipe wall results in the formation of a streaming potential that causes a return current to flow through both the solution and the conducting walls of the pipe. These are steady-state currents that arise to maintain over-all charge balance, and are not involved with any net work being done. Under conditions where the flow is accelerating, however, it has been proposed that the localized divergence of fluid velocity where the flow is accelerating results in divergence of the current. In this case, charge balance is restored by an additional current arising from oxidation/reduction reactions taking place at the surface. This phenomenon was proposed by Beck *et al*. [110] to account for pitting of aircraft slide and sleeve hydraulic servo valves in a phosphate ester base hydraulic fluid, where the acceleration of the fluid through a gap at the interface of the slide and sleeve formed an anodic region on the surface of the sleeve and caused pitting of the sleeve. In the case of the fouling of flow orifices by magnetite, it is proposed that the acceleration of the fluid as it enters the orifice results in the formation of an anodic region at the entrance to the orifice and precipitation of magnetite via oxidation of ferrous ions [111, 112].

There has been a renewal of interest in the possible link between electrokinetic potentials and the accumulation of deposit in regions of accelerating flow in response to the experience of flow blockage of quatrefoils which lead to SG tube failures at some plants operated by EdF [38, 39]. Investigations by Guillodo *et al*. [114, 115] and Barale *et al*. [116, 117] conducted in fast-flowing water (fluid velocity ≈ 10 m/s) under secondary chemistry conditions have reproduced the previous results of Woolsey *et al*. [111]. Guillodo *et al*. considered three mechanisms that could potentially contribute to deposit formation [115]:

1) electrokinetic effects [110, 111, 112],
2) flashing [67, 68, 108], and
3) particle trapping [67, 68].

Mechanisms 1 and 2 were considered to be the most plausible, and were consistent with inspections of TSP blockage. Mechanism 3 was disregarded because it was not supported by inspection of the TSPs. Loop tests showed evidence for both precipitation fouling and deposition of fine particles within the orifice. The investigators proposed that pH and a redox potential were both important parameters, suggesting that a pH_T in the vicinity of 5.7 to 5.9 and a redox potential more positive than -570 mV relative to an Ag-AgCl electrode promoted fouling of the orifice. Although providing valuable data and information for understanding and controlling deposition in TSPs, their studies did not provide a definitive answer as to the extent to which electrokinetic potential contributed to deposition. Barale *et al.* also found that redox potential is a major parameter affecting deposit formation in a flow orifice. Their studies found that deposit accumulation occurred for a redox potential (relative to Ag-AgCl) more positive than -530 mV for nickel-base alloys and more positive than -450 mV for 410 stainless steel [117]. No definitive statement was made, however, regarding the contribution of electrokinetic potential to the deposition observed.

TABLE 3: Approximate Distribution of Iron Transported with the Feed Water to an RSG

Tube-bundle deposit	~70%
Tube-sheet deposit	~15%
Removed by blow down	~15%

4. Plant Experience with Fouling Mitigation: Alternative Amines, Filming Amines and Chemical Dispersants

4.1 Criterion for Evaluating the Impact of Water Treatment Chemicals on the Rate of SG Fouling

Corrosion products that are transported to the SG with the feed water either accumulate within the SG by deposition onto an internal surface, e.g., primarily the tube-bundle, the tube-sheet and tube-support structure, or they remain suspended in the recirculating water where they are removed from the SG via blow down or moisture carry-over.[14] Table 3 lists the approximate distribution of corrosion products between various 'sinks' as a percentage of the total iron transported to the SGs with the feed water during operation. The estimated distribution listed in Table 3 is based on data from tube-sheet sludge lancing and chemical cleaning campaigns [118, 119, 120], and measurements of tube deposit loading [121] and corrosion product transport in the feed water and blow down [9, 122, 123].

It is clear from Table 3 that the fouling of internal surfaces

[14] Blow down is defined in Section 2.1. Moisture carry-over refers to the water content of the main steam exiting an RSG.

within the SG, and especially the accumulation of deposit on the tube-bundle, is a more effective removal mechanism for suspended corrosion product than removal from the SG by blow down. In other words, the fact that only 15% (on average) of the corrosion product that is transported to the SG during operation is removed by blow down is a direct consequence of the fact that the rate of removal of corrosion product via fouling of the tube-bundle is higher than the rate of removal by blow down. It follows that a water treatment chemical that results in a reduction in the tube-bundle fouling rate will lead to an increase in blow down efficiency and vice versa, as discussed below.

The fact that fouling of the internal surfaces of a SG is a more effective removal mechanism for corrosion products than blow down is related to the relative time scales on which the two processes occur. This is illustrated by comparing the half-mean-life for removal of corrosion product from the SG by blow down to the half-mean-life for removal of corrosion product from suspension by fouling, as shown by the following analysis [6].

The half-mean-life for removal of corrosion products from a SG via blow down is given by:

$$t_{1/2} = 0.5 * M / BD \quad (25)$$

Equation (25) says that the half-mean-life for removal of suspended corrosion products from a SG by blow down is proportional to the total mass of fluid in the SG and inversely proportional to the blow down flow rate. For example, the half-mean-life for removal of suspended corrosion products from a CANDU 6 SG with a blow down flow rate of 1.3 kg/s, i.e., 0.5% of the steaming rate, and an inventory of 50 Mg of water during operation at power is 5.1 hours. Similarly, the half-mean-life for removal of corrosion products by fouling of the SG is given by:

$$t_{1/2} = 0.5 * M / (\rho K_f * A) \quad (26)$$

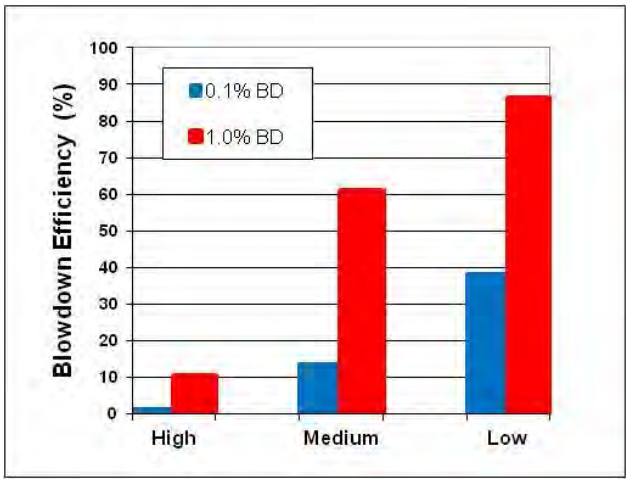

FIGURE 15: Effect of fouling rate on blow down efficiency (%) for two different blow down rates from simulations of fouling of an RSG using the SLUDGE code.

Thus, the fouling half-mean-life is inversely proportional to the product of the overall fouling rate constant and the surface area on which deposit accumulates. Considering only tube-bundle fouling, half-mean-lives for tube-bundle fouling for magnetite and hematite, calculated using the fouling rate constants shown in Figures 11 and 12, respectively, and a tube-bundle surface area of 3,500 m^2, are listed in Table 4 for selected amines.

For situations where $t_{1/2\ fouling} \approx t_{1/2\ blow\ down}$, i.e., fouling of magnetite in the presence of morpholine or ETA, the suspended corrosion products have approximately equal chances of being removed from the SG by blow down and being removed from suspension by fouling of the tube-bundle. Alternatively, if $t_{1/2\ fouling} >> t_{1/2\ blow\ down}$, i.e., fouling of magnetite in the presence of DMA or a mixture of ETA

TABLE 4: Calculated Fouling Half-Mean-Lives for Magnetite and Hematite Based on Fouling Rates Reported in Figure 11 and Figure 12

ρK_f (kg/m^{2}s)	Amine	$t_{1/2}$ (fouling) (hours)
Magnetite		
3.48×10^{-4}	Morpholine	5.7
5.52×10^{-4}	ETA	3.6
1.16×10^{-4}	DMA	17
0.7×10^{-4}	DDA/ETA	28
Hematite		
1.82×10^{-2}	Morpholine	0.11
1.08×10^{-2}	ETA	0.18
0.153×10^{-2}	DMA	1.29
-	DDA/ETA	-

and DDA, the particles will remain in suspension longer, which increases the likelihood of the corrosion products being removed from the SG by blow down. Conversely, if $t_{1/2\ fouling} << t_{1/2\ blow\ down}$, i.e., fouling by hematite in the presence of morpholine or ethanolamine, the rate of tube-bundle fouling is so high that the particles do not remain suspended long enough to have much chance of being removed from the SG by blow down.

The inverse relationship between tube-bundle fouling rate and blow down efficiency is illustrated by the results from modelling particulate fouling of an RSG shown in Figure 15. The figure shows the expected blow down efficiency versus fouling rate for two different blow down rates based on simulations of RSG fouling using a three-dimensional transient fouling code (SLUDGE) developed by Atomic Energy of Canada Limited (AECL). The fouling simulations were based on a CANDU 6 SG using a particle size of 1 μm. The blow-down flow rate is expressed as a percentage of the steaming rate. The concentration of suspended corrosion product in the SG recirculating water is a steady-state between the rate of input of corrosion product to the SG and the rates of removal by blow down and by fouling of the internal surfaces of the SG, as described elsewhere [121].

For the simulation results shown in Figure 15, a medium fouling rate corresponds to deposition of magnetite under flow-boiling conditions using morpholine to adjust the pH (see Figure 11). High and low fouling rates were arbitrarily selected to be 10-times higher and 10-times lower than the medium fouling rate, respectively. The results of the simulations show that a reduction in the tube-bundle fouling rate will be manifested by an increase in the blow down efficiency, a result that is consistent with the argument above based on the relative half-lives for blow down and tube-bundle fouling.

The discussion in this section has shown that the overall SG fouling rate is inversely proportional to the blow down efficiency. It follows, therefore, that a reduction in the SG fouling rate for a given rate of iron transport to the SG will be manifested by an increase in blow down efficiency and *vice versa*.

4.2 Alternative Amines

No systematic assessment has been published in the open literature on the effect of various alternative amines used for pH-control in the secondary systems of nuclear SGs on the rate of SG fouling using the criterion discussed in Section 4.1. There are numerous papers on the effect of alternative amines on the rate of iron transport to the SGs, and while this is of prime concern to power plant operators these reports tend not to include sufficient information to deduce an amine-specific effect on the rate of SG fouling, as might be expected from the data shown in Figures 11 and 12.

One study has been published that looked for evidence from operating-plant data for a dimethylamine (DMA)-specific effect on both the rate of FAC and the rate of SG fouling [124]. This assessment focussed on nine plants operating in the U.S. that had initiated the addition of DMA after at least one cycle of operation. The evaluation of whether the addition of DMA to the feedwater system had any influence on the subsequent rate of SG fouling was based on an examination of trends of either the main-steam pressure or the SG fouling factor, as determined by a fouling factor analysis [26]. Unfortunately, the impact of the addition of DMA on blow-down efficiency was not included in the assessment.

Although the thermal fouling trend is important from the perspective of plant performance, it does not unambiguously provide a measure of the rate of accumulation of deposit on the SG tube-bundle. Several additional factors, including tube-deposit density and morphology, separator fouling, reactor power and primary coolant temperature, also influence the magnitude of the thermal fouling factor derived from plant-operating data, and care must be taken to separate these effects from the effect of deposit accumulation itself[15]. The methodology used to derive the thermal fouling factor is particularly important when comparing trends from one plant to another [25, 26]. The methodology used to calculate fouling factor trends was not described in the published report, and in only one case was it noted that the fouling factor was corrected for changes in reactor power level and the primary coolant temperature. Although the report concluded that no DMA-specific effect on the rate of SG fouling was apparent from the plant data, it is suggested here that the lack of rigour in comparing thermal performance trends from one plant to another and the absence of more definitive information on blow-down efficiency make the results of this assessment inconclusive.

4.3 Filming Amines

As noted in Section 3.3.2.3, there is increasing interest in the use of filming amines to mitigate corrosion in the steam cycle and fouling in nuclear SGs. Filming amines have used since the 1960s to mitigate corrosion in steam condensate systems in numerous industrial applications [125, 126], where their effectiveness is proposed to be related to the establishment of a non-wettable film on metal surfaces [126]. The film is proposed to be monolayer in thickness, and so its effectiveness does not increase with continued treatment beyond that required to maintain the monolayer coverage of the system surfaces. The most effective filming amines are those aliphatic amines with 10 to 18 carbon atoms in the chain. Octadecylamine (ODA) is a commonly used filming amine for the protection of industrial condensate systems.

The addition of ODA to mitigate corrosion in the secondary

[15] For CANDU plants that use carbon steel in the reactor-coolant circuit, the additional thermal resistance attributable to fouling of the inside surface of the SG tubes is a further complicating factor [25].

system and SGs of VVER plants is being investigated by a combination of experiments in autoclaves and tests in a pilot-scale SGs [127]. Its effectiveness is being evaluated with respect to its ability to mitigate FAC in the steam cycle to reduce the level of corrosion product transport to the SGs during power operation, as well as to reduce the risk of chloride cracking of the stainless steel SG tubes. The test program showed that ODA reduced the rate of chloride-cracking of stainless steel. It was postulated that its effectiveness was related to its adsorption onto the surface of the stainless steel, thus preventing access to the surface by chloride. Although the investigation was focussed on the effectiveness of ODA at mitigating corrosion, it was noted that the application of ODA to the Kola NPP increased the operating period between chemical cleanings. No other details were provided in the paper, so it is not clear whether the reduction in SG fouling was due to reduced corrosion product transport, reduced SG fouling or some combination of the two. In other testing in the pilot-scale SG, the application of ODA reduced tube deposits from an average loading of 48 g/m^2 to 17 g/m^2. Although few details were provided regarding deposit characterization, it appears that the application of ODA has been effective at removing deposit from the SG tube-bundle under SG operating conditions.

Results from field trials of the use of filming amines to mitigate corrosion in the steam cycles of PWR plants have been reported recently [128, 129]. As with the ODA trial reviewed above, the motivation for adding the filming amine was the reduction of FAC in the steam-cycle piping and, thereby, a reduction of the corresponding rate corrosion product transport to the SGs. Significantly, the field-trial results showed both a reduction in feed-water iron transport to the SGs and an increase in the concentration of corrosion product in the SG blow down, i.e., an increase in blow-down efficiency. This is a very important observation because it implies that the addition of the filming amine has reduced the rate of fouling of the SGs. Although it is possible that some of the increase in the concentration of corrosion product in the blow down arises from the removal of deposit from within the SG, it is more likely that the major contributing factor is a reduction in the rate of tube-bundle fouling.

4.4 Chemical Dispersants

While polymeric dispersants have been used for decades to mitigate deposit accumulation in fossil fuelled SGs, the nuclear industry has been reluctant to introduce dispersants to nuclear SGs to mitigate fouling because of the possibility of introducing inorganic impurities (left over from the polymer synthesis) to the SGs, and concerns regarding the impact of polymer decomposition products on crevice chemistry and materials. The CANDU Owners Group funded research to investigate the feasibility of applying dispersants to CANDU SGs, and made preparations for a field trial of a low molecular weight PAA dispersant [105, 106]. The program was stopped, however, before a field trial could be launched. Betz Dearborn developed a high molecular weight PAA dispersant for application in nuclear SGs. Following rigorous qualification [130] the dispersant was approved for use, first in a short-term trial at ANO-2 [131] and subsequently at a longer-term trial at McGuire 2 [132].

The short-term trial at ANO-2 successfully demonstrated that PAA could mitigate deposition in nuclear SGs. PAA was added to the feedwater at a concentration of 2 µg/kg at the beginning of the trial, and the concentration was raised incrementally to 12 µg/kg by the end of the trial. Blowdown efficiencies for the two SGs increased from pre-trial values of 1 to 2% to average values of 20 to 60% during the trial. There were no unexpected changes in secondary system chemistry that were attributed to PAA addition to the feedwater. Changes in cation conductivity and total organic carbon were observed, but these correlated with changes in the concentration of ethanolamine, which is added for pH control at ANO-2. Analysis of the thermal-hydraulic performance of the plant suggested that the feedwater venturis de-fouled during the injection of dispersant while the steam venturis appear to have fouled. One apparently adverse effect of the dispersant addition was the sharp loss of thermal performance of the SGs during the last six weeks of the trial which was only partially recovered when dispersant injection was stopped at the end of the trial. Two plausible causes of the loss of thermal performance were suggested: fouling of the moisture separators and loss of the porous outer layer of deposit on the tube-bundle.[16] Of these two factors, loss of the porous outer layer was suggested to be the more likely [133], although this explanation does not account for the observation that the loss took place primarily during the last six weeks of the trial. Fouling of both the moisture separators and the steam venturis is consistent with the high moisture carry-over-rate of 1% at ANO-2. With blow-down iron concentrations averaging 14 to 32 times higher during the trial compared to pre-trial values[17], the fouling rates of any components exposed to high-pressure steam will be correspondingly higher during PAA injection. The rate of moisture carry-over at ANO-2 is anomalously high, and so the effect of elevated suspended iron concentration in the SG on the fouling of steam-cycle components down stream of the SGs will be significantly

[16] The outer porous layer reduces the wall superheat required for bubble nucleation, hence, acts to increase the rate of heat transfer. Only the dense inner layer offers a resistance to heat transfer.
[17] A log mean average is reported in Reference [131].

higher at ANO-2 than at other plants. Fouling of steam-cycle components is not expected to affect performance at plants where the rate of moisture carry-over is not an issue.[18]

The short term trial at ANO-2 was followed by a longer term trial at McGuire-2. PAA was injected into the feedwater to achieve a feedwater concentration ranging from 0.5 to 4 μg/kg. Blow-down efficiency increased from a pre-trial value of 5% to values in the range 45 to 50% when the PAA concentration was maintained between 2 and 4 μg/kg, i.e., roughly equivalent to the feed-water total iron concentration. It was reported that none of the secondary-system chemistry parameters were adversely affected during the trial. Exelon is implementing online PAA dispersant technology at Braidwood Units 1 and 2 and at Byron Units 1 and 2. Preliminary results are encouraging, with iron blow-down efficiencies at both Braidwood and Byron increasing to more than 50% [133, 134].

5. Summary and Conclusions

Fouling remains a potentially serious issue that if left unchecked can lead to degradation of the safety and performance of nuclear SGs. It has been demonstrated that the majority of the corrosion product transported with the feed water to the SGs accumulates in the SG on the tube-bundle. By increasing the risk of tube failure and acting as a barrier to heat-transfer, deposit on the tube-bundle has the potential to impair the ability of the SG to perform its two safety critical roles: provision of a barrier to the release of radioactivity from the reactor coolant and removal of heat from the primary coolant during power operation and under certain post accident scenarios. Thus, it is imperative to develop improved ways to mitigate SG fouling for the long-term safe, reliable and economic performance of NPPs.

Fifty years ago, the understanding of heat exchanger fouling was largely phenomenological, based on little or no mechanistic information. The impact of fouling on heat-exchanger performance was accounted for by adding a "fouling factor" to the heat-transfer calculation so the heat exchanger could be properly sized to take account of the impairment of heat-transfer by fouling. For the design of heat-exchanger equipment used in aqueous systems, the first edition of the Tubular Exchanger Manufacturers Association (TEMA) tables of fouling factors applicable to shell and tube heat exchanger equipment lists fouling factors for the following types of cooling water: sea water, brackish water, muddy water, river water, etc. [135]. Different fouling factors are suggested depending on whether the temperature is greater than or less than ~ 50 °C and whether the fluid velocity is greater than or less than ~ 1 m/s.

Significant progress has been made in developing a mechanistic understanding of the fouling of heat exchangers over the past five decades. As discussed in this paper, particulate fouling is now understood in terms of a process involving particle transport, attachment, removal and consolidation on the heat-transfer surface. Correlations have been developed that have been shown to give good agreement with experimental data for the transport of fine particles (~1 μm) from the bulk to the heat-transfer surface in aqueous systems. The effect of water chemistry on the rate of particulate fouling by corrosion products is described by taking account of the effect of pH on the surface potentials of both the corrosion products and the surface on which they are depositing. Advances have been made in understanding the influence of boiling on the rate of particulate fouling by probing the nature of the particle-bubble interaction and how this interaction contributes to the accumulation of particles at bubble nucleation sites. Water chemistry has been shown to exert a strong influence on the rate of particulate fouling under flow-boiling conditions. For example, the amine used to control the pH has been shown to have a strong effect on the fouling rate, quite apart from any effect of pH. A class of amine known as filming amines appears to be particularly effective at reducing the particulate fouling rate under flow-boiling conditions, and, of course, dispersants have been used in industrial boilers for years to mitigate fouling. These latter chemicals are just starting to be introduced for use with nuclear SGs, and promise to be effective tools for the mitigation of the fouling of nuclear SGs.

Alternative amines, filming amines and dispersants all hold good promise for the development of improved water treatment strategies to mitigate the fouling of SGs, and especially fouling of the tube-bundle. How these reagents act to mitigate fouling, however, is not well understood. Further research is needed to better understand why some amines, for example, DMA, are effective at reducing the rate of deposit consolidation, thereby making it easier to remove particles that have already deposited and reducing the overall rate of fouling. The mechanism by which filming amines and dispersants act to reduce the fouling rate in boiling water is also not well understood. It is known from previous investigations that dispersants that are effective at mitigating fouling under flow-boiling heat-transfer are not necessarily effective when heat-transfer is by single-phase forced convection. This result focuses attention on the bubble-nucleation process itself, and how it affects the rate of particulate fouling. Further research into the influence of filming amines and dispersants on bubble-nucleation and growth, the particle-bubble interaction and subsequent accumulation of particles at bubble-nucleation sites should prove beneficial towards developing a better understanding of why these reagents are effective at mitigating particulate fouling in flow-boiling systems and how to develop new and improved water-treatment chemistries to mitigate the fouling of SGs.

[18] Moisture carry over rates at plants with properly functioning moisture separators are generally < 0.25%.

References

[1] International Atomic Energy Agency, 1997, "Assessment and Management of Ageing of Major Nuclear Power Plant Components Important to Safety: Steam Generators", Report IAEA-TECDOC-981.
[2] J. Riznic and S. Milivojevic, 2006, "Some Performance Indicators of PWR Steam Generators", Proceedings of the 5th Canadian Nuclear Society International Steam Generator Conference, Toronto, Canada, 2006 November 26-29.
[3] R.L. Tapping, J. Nickerson, P. Spekkens, and C. Maruska, 2000, "CANDU Steam Generator Life Management", Nuclear Engineering and Design, 197(1), pp. 213-223.
[4] R.W. Staehle, J.A. Gorman, A. McIlree and R.L. Tapping, 2006, "Status and Future of Corrosion in PWR Steam Generators", Presented at Fontrevaud 6, Fontrevaud Royal Abbey, France, 2006 September 18-22, Paper A106-T06.
[5] B. Lukasevitch, N. Trunov, V. Sotskov and S. Harchenko, 2006, "The Past and the Future of Horizontal Steam Generators", Proceedings of the 5th Canadian Nuclear Society International Steam Generator Conference, Toronto, Ontario, Canada, 2006 November 26-29.
[6] C.W. Turner, 2011, "Implications of Steam Generator Fouling on the Degradation of Material and Thermal Performance", Proceedings of the 15th International Conference on the Environmental Degradation of Materials in Nuclear Reactor Systems, Colorado Springs, Colorado, USA, August 7-11, 2011, pp. 2287-2299.
[7] J.A. Sawicki and M.E. Brett, 1993, "Mossbauer Study of Corrosion Products from a CANDU Secondary System", Nuclear Instruments and Methods in Physics Research B76(1-4), pp. 254-257.
[8] "Pressurized Water Reactor Secondary Water Chemistry Guidelines-Revision 7", Electric Power Research Institute Final Report 1016555, February 2009.
[9] J.A. Sawicki, M.E. Brett and R.L. Tapping, 1998, "Corrosion-Product Transport, Oxidation State and Remedial Measures", Atomic Energy of Canada Report AECL-11959, COG-98-314-I, 1998 October.
[10] P.J. Millett and S.G. Sawochka, 1994, "Investigation of Redox Conditions in the Secondary System of PWRs", Proceedings of Chemistry in Water Reactors: Operating Experience and New Developments, Nice, France, April 24-27, 1994, pp. 618-622.
[11] A.A. Efimov, L.N. Moskvin, G.N. Belozerskii, M.I. Kazakov, B.A. Gusev, and A.V. Semenov, 1989, "Mössbauer Phase Analysis of Corrosion Products Dispersed in Nuclear Power Station Coolant", Atomnaya Energiya, 67(6), pp. 389-392.
[12] G.A. Sehmel, 1970, "Particle Sampling Bias Introduced by Anisokinetic Sampling and Deposition Within the Sampling Line", American Industrial Hygiene Association Journal, 31(6), pp. 758-771.
[13] V. Vitols, 1966, "Theoretical Limits of Errors due to Anisokinetic Sampling of Particulate Matter", Journal of the Air Pollution Control Association, 16(2), pp. 79-84.
[14] E.J. Bird, 1984, "Experience of Continuous Isokinetic Sampling on the Winfrith Reactor", Proceedings: Workshop on Corrosion Product Sampling From Hot Water Systems, Electric Power Research Institute Report EPRI NP-3402-SR, March 1984, pp.2-1 – 2-19.
[15] P. Srisukvatananan, D.H. Lister, R. Svoboda and K. Daucik, 2007, "Assessment of the Sate of the Art of Sampling of Corrosion Products from Water/Steam Cycles", Power Plant Chemistry, 9(10), pp. 613-626.
[16] P. Srisukvatananan, D.H. Lister, C.E. Ng, R. Svoboda, and K. Daucik, 2008, "Corrosion Product Sampling in Power Plants under Water/Steam Cycle Conditions", Proceedings on the 15th International Conference on the Properties of Water and Steam, Berlin, Germany.
[17] C.C. Stauffer, 1984, "Corrosion Product Sampling Experience at Babcock and Wilcox", Proceedings: Workshop on Corrosion Product Sampling From Hot Water Systems, Electric Power Research Institute Report EPRI NP-3402-SR, March 1984, pp. 7-1 – 7-23.
[18] G.F. Palino, D. McNea and W.R. Kassen, 2000, "Design of PWR Reactor Coolant Hot Sample Panel for Diablo Canyon", Electric Power Research Institute Report 1000990, December 2000.
[19] J. Sawicki, 1999, "Proceedings of the COG Workshop on Layup, Shutdown and Startup Chemistry Optimization", CANDU Owners Group Report COG-00-066-I, 1999 March
[20] K. Verma, S. Odar and D. Scott, 1996, "Steam Generator Secondary Side Chemical Cleaning at Point Lepreau using the Siemen's High Temperature Process", Presented at the 4th Technical Committee Meeting on the Exchange of Operational Safety Experience of Pressurized Heavy Water Reactors, Kyong-Ju, Korea, April 21-26, 1996.
[21] S. Plante, 2005, "Steam Generator Secondary Side Chemical Cleaning at Gentilly-2", Proceedings of the Seventh CNS International Conference on CANDU Maintenance, Toronto, Ontario, Canada, November 20-22, 2005.
[22] J. Taborek, T. Aoki, R.B. Ritter, and J.W. Palen, 1972, "Fouling: The Major Unresolved Problem in Heat-transfer", Chemical Engineering Progress, 68(2), pp. 59-67.
[23] C.W. Turner, S.J. Klimas, and M.G. Brideau, 2000,"Thermal Resistance of Steam-Generator Tube Deposits under Single-Phase Forced Convection and Flow-Boiling Heat-transfer", Canadian Journal of Chemical Engineering, 78(2), pp. 53-60.
[24] J.T. Lovett and B.L. Dow, 1991, "Steam Generator Performance Degradation", Electric Power Research Institute Report NP-7524.
[25] M. Yetisir, C.W. Turner and J. Pietralik, 2000, "Contribution of SG Degradation Mechanisms to RIHT Behaviour", Proceedings of the Fifth CANDU Maintenance Conference, Toronto, Ontario, Canada, November 19-21, 2000, pp. 319-326.
[26] M. Kreider, G.A. White, and R.D. Varrin, Jr., 1998, "A Global Fouling Factor Methodology for Analyzing Steam Generator Thermal Performance Degradation", Third International Steam Generator and Heat Exchanger Conference, Toronto, Ontario, Canada, June 1998, pp.191-208.
[27] 1994, Steam Generator Progress Report, Revision 10, Energy Management Services, Inc., Little Rock, Arkansas, November 1994.
[28] P.V. Balakrishnan, S.M. Pagan, S.M. McKay and F. Gonzalez, 1996, "Hideout and Hideout Return: Laboratory Studies and Plant Measurements", CANDU Owners Group Report COG-95-555-I, 1996 May.
[29] P.V. Balakrishnan, 1999, "Hideout, Hideout Return and Crevice Chemistry in Steam Generators", Proceedings of the Thirteenth International Conference on the Properties of Water and Steam, Toronto, Ontario, Canada, September 12-16, 1999, pp. 858-865.
[30] Y. Lu, 2007, "Define Optimal Conditions for Steam Generator Tube Integrity and an Extended Steam Generator Service Life", 15th International Conference on Nuclear Engineering ICONE-15, Nagoya, Japan, April 2007, Paper ICONE15-10854.
[31] H.E.C. Rummens, 1999, "The Thermalhydraulics of Tube-Support Fouling in Nuclear Steam Generators", PhD Thesis, Carleton University, Ottawa, Canada.
[32] L.E. Johnson, 1987, "Fouling in Nuclear Once-Through Steam Generators", Paper 87-WA/NE-12, ASME Winter Annual Meeting, Boston, Massachusetts, USA.
[33] R.H. Thompson and L.S. Lammana, 1986, "Video Inspection and Sampling of the Crystal River Unit-3 Once-Through Steam Generators", Proceedings of the Fourty-seventh International Water Conference, Pittsburgh, Pennsylvania, Paper IWC-86-3, pp.9-16.
[34] R.H. Thompson, 1992, "Fouling of the Crystal River-3 Once-Through Steam Generators After Switchover to Morpholine Water Chemistry", Proceedings of the 1992 International Joint Power Generation Conference, Atlanta, ASME NE-Volume 8, pp. 29-38.
[35] M.M. Stickel, E.P. Morgan, M.H. Hu, H.L. Miller and J.O. Eastwood, 1994, "Steam Generator Water Level Oscillations Resulting from Sludge Induced Flow Blockage", Proceedings: Steam Generator Sludge Management Workshop, Norfolk, Virginia, EPRI Report TR-104212, pp. 15-1 – 15-33.
[36] R. Dyck, P. Spekkens, K. Verma, and A. Marchand, 1990, "Operational Experience with Steam Generators in Canadian Nuclear Plants", Proceedings of the Steam Generator and Heat Exchanger Conference, Toronto, Ontario, Canada, April-May 1990, pp. 1-10 – 1-127.
[37] J. Malaugh and S. Ryder, 1990, "Bruce NGS-A Support Plate Inspection and Waterlancing", Proceedings of the Steam Generator and Heat Exchanger Conference, Toronto, Ontario, Canada, April-May 1990, pp. 3-51 – 3-76.
[38] H. Bodineau and T. Sollier, 2008, "Tube-support Plate Clogging Up of French PWR Steam Generators", Eurosafe 2008 Forum, Paris, France.
[39] G. Corredera, M. Alves-Vieira and O. De Bouvier, 2008, "Fouling and TSP Blockage of Steam Generators on EDF Fleet: Identified Correlation with Secondary Water Chemistry and Planned Remedies", International Conference on Water Chemistry of Nuclear Reactor Systems, Berlin, Germany, September 15-18, 2008.
[40] P. Luna, G. Diaz, H. Sveruga and R. Sainz, 2006, "Maintenance and Life

Assessment of Steam Generators at Embalse Nuclear Station", Proceedings of the 5th Canadian Nuclear Society International Steam Generator Conference, Toronto, Ontario, Canada, November 26-29, 2006.
[41] L. Obrutsky, R. Cassidy, M. Cazal and K. Sedman, 2006, "Eddy Current Assessment of Support Plate Structures Degradation in Nuclear Steam Generators", 5th Canadian Nuclear Society International Steam Generator Conference, Toronto, Ontario, Canada, November 26-29, 2006.
[42] K.G. Sedman, G.E. Galan and B. Dicks, 2005, "Boiler Tube-support Plate Degradation in Bruce Unit 8", Proceedings of the Seventh Canadian Nuclear Society International Conference on CANDU Maintenance, Toronto, Ontario, Canada, November 20-22, 2005.
[43] N. Epstein, 1983, "Thinking about Heat-transfer Fouling: A 5 x 5 Matrix", Heat-transfer Engineering, 4(1), pp. 43-56.
[44] J.S. Gudmundsson, 1981, "Particulate Fouling", Fouling of Heat-transfer Equipment, Editors E.F.C. Somerscales and J.G. Knudsen, Hemisphere, Washington D.C., pp. 357-387.
[45] A.B. Metzner and W.L. Friend, 1958, "Theoretical Analogies between Heat, Mass and Momentum Transfer and Modifications for Fluids of High Prandtl or Schmidt Numbers", The Canadian Journal of Chemical Engineering, 36(6), pp. 235-240.
[46] J.W. Cleaver and B. Yates, 1975, "A Sub Layer Model for the Deposition of Particles from a Turbulent Flow", Chemical Engineering Science, 30(8), pp. 983-992.
[47] S.K. Friedlander and H.F. Johnstone, 1957, "Deposition of Suspended Particles from Turbulent Gas Streams", Industrial & Engineering Chemistry, 49(7), pp. 1151-1156.
[48] M.W. Reeks and G. Skyrme, "The Dependence of Particle Deposition Velocity on Particle Inertia in Turbulent Pipe Flow", 1976, Journal of Aerosol Science, 7(6), pp. 485-495.
[49] A. Guha, 1997, "A Unified Eulerian Theory of Turbulent Deposition to Smooth and Rough Surfaces", Journal of Aerosol Science, 28(8), 1517-1537.
[50] P.G. Papavergos and A.B. Hedley, 1984, "Particle Deposition Behaviour from RidgeTurbulent Flows", Chemical Engineering Research and Design, 62(5), pp. 275-295.
[51] A.M. Reynolds, 1999, "A Lagrangian Stochastic Model for Heavy Particle Deposition", Journal of Colloid and Interface Science, 215(1), pp. 85-91.
[52] C.W. Turner, 1993, "Rates of Particle Deposition from Aqueous Suspensions in Turbulent Flow: A Comparison of Theory with Experiment", Chemical Engineering Science, 48(12), pp. 2189-2195.
[53] N. Epstein, 1981, "Fouling: Technical Aspects (Afterword to Fouling in Heat Exchangers)", Fouling of Heat-transfer Equipment, Editors E.F.C. Somerscales and J.G. Knudsen, Hemisphere, Washington D.C., pp. 31-53.
[54] E. Ruckenstein and D.C. Prieve, 1973, "Rate of Deposition of Brownian Particles Under the Action of London and Double-Layer Forces", Journal of the Chemical Society, Faraday Transactions II, 69, pp. 1522-1536.
[55] P.C. Hiemenz and R. Rajagopalan, 1997, "Principles of Colloid and Surface Chemistry", 3rd Rev. Ed., Marcel Dekker, Inc., New York.
[56] G.A. Parks and P.L. de Bruyn, 1962, "The Zero Point of Charge of Oxides", Journal of Physical Chemistry, 66(6), pp. 967-973.
[57] J.W. Cleaver and B. Yates, 1973, "Mechanism of Detachment of Colloidal Particles from a Flat Substrate in a Turbulent Flow", Journal of Colloid and Interface Science, 44(3), pp. 464-474.
[58] M.E O'Neill, 1968, "A Sphere in Contact with a Plane Wall in a Slow Linear Shear Flow", Chemical Engineering Science, 23(11), pp. 1293-1298.
[59] P.G. Saffman, 1965, "The Lift on a Small Sphere in a Slow Shear Flow", Journal of Fluid Mechanics, 22(2), pp. 385-400.
[60] B.P.K. Yung, H. Merry,and T.R. Bott, 1989, "The Role of Turbulent Bursts in Particle Re-Entrainment in Aqueous Systems", Chemical Engineering Science, 44(4), pp. 873-882.
[61] J.W. Cleaver and B. Yates, 1976, "The Effect of Re-Entrainment on Particle Deposition", Chemical Engineering Science, 31(2), pp. 147-151.
[62] C.W. Turner, M.E. Blimkie and P.A. Lavoie, 1997, "Physical and Chemical Factors Affecting Sludge Consolidation", Atomic Energy of Canada Report AECL-11674, COG-96-492-I, 1997 September.
[63] C.W. Turner and S.J. Klimas, 2001, "The Effect of Surface Chemistry on Particulate Fouling under Flow-Boiling Conditions", Proceedings of Heat Exchanger Fouling: Fundamental Approaches and Technical Solutions, Davos, Switzerland. AECL-12171.
[64] A.W. Adamson, 1982, "Physical Chemistry of Surfaces", Fourth Edition, John Wiley & Sons, New York.
[65] C.W. Turner and D.W. Smith, 1998, "Calcium Carbonate Scaling Kinetics Determined from Radiotracer Experiments with Calcium-47", Industrial & Engineering Chemistry Research, 37(2), pp. 439-448. AECL-11906
[66] S.J. Klimas, D.G. Miller, J. Semmler, and C.W. Turner, 1998, "The Effect of the Removal of Steam Generator Tube ID Deposits on Heat-transfer", Third International Heat Exchanger and Steam Generator Conference, Toronto, Ontario. AECL-11985.
[67] H.E.C. Rummens and C.W. Turner, 1994, "Experimental Studies of Flow Pattern Near Tube-support Structures", Proceedings of the 2nd International Steam Generator and Heat Exchanger Conference, Toronto, Ontario. AECL-11145, COG-94-361.
[68] H.E.C. Rummens, J.T. Rogers and C.W. Turner, 2004, "The Thermal Hydraulics of Tube-support Fouling in Nuclear Steam Generators", Nuclear Technology, 148(3), pp. 268-286.
[69] C.W. Turner, D.A. Guzonas and S.J. Klimas, 2004, "Surface Chemistry Interventions to Control Boiler Tube Fouling – Part II", Atomic Energy of Canada Limited Report AECL-12100, 2004 June.
[70] D.Q. Kern and R.E. Seaton, 1959, "A Theoretical Analysis of Thermal Surface Fouling", British Chemical Engineering, 4(5), pp. 258-262.
[71] G.S. McNab and A. Meisen, 1973, "Thermophoresis in Liquids", Journal of Colloid and Interface Science, 44(2), pp. 339-346.
[72] C.W. Turner and D.W. Smith, 1992, "A Study of Magnetite Particle Deposition onto Alloy-800 and Alloy-600 between 25 and 80 °C and predicted rates under steam generator operating conditions", Proceedings of Steam Generator Sludge Deposition in Recirculating and Once Through Steam Generator Upper Tube-bundle and Support Plates, Editors R.L. Baker and E.A. Harvego, Atlanta, ASME NE, 8, pp. 9-18. AECL-10754, COG-92-344.
[73] D.H. Lister and F.C. Cussac, 2007, "Modelling of Particulate Fouling on Heat Exchanger Surfaces: Influence of Bubbles on Iron Oxide Deposition", Proceedings of the Seventh International Conference on Heat Exchanger Fouling and Cleaning - Challenges and Opportunities 2007, Editors Hans Muller-Steinhagen, M. Reza Malayeri and A. Paul Watkinson, Engineering Conferences International, Tomar, Portugal, pp. 268-277.
[74] A.P. Watkinson and N. Epstein, 1970, "Particulate Fouling of Sensible Heat Exchangers", Proceedings of the Fourth International Heat-transfer Conference, Versailles, France, Volume 1, Paper HE1.6.
[75] R.M. Hopkins and N. Epstein, 1974, "Fouling of Heated Stainless Steel Tubes by a Flowing Suspension of Ferric Oxide in Water", Proceedings of the Fifth International Heat-transfer Conference, Tokyo, Japan, Volume 5, pp. 180-184.
[76] J.S. Gudmundsson, 1977, "Fouling of Surfaces", Ph.D. Thesis, University of Birmingham.
[77] I.H. Newson, 1979, "Studies of Particulate Deposition from Flowing Suspension", Fouling - Science or Art?, University of Surrey, pp. 35-81.
[78] I.H. Newson, T.R. Bott, and C. Hussain, 1981, "Studies of Magnetite Deposition from a Flowing Suspension", Fouling in Heat Exchange Equipment, ASME Heat-transfer Division, Publication HTD Volume 17, pp. 73-81.
[79] I.H. Newson, T.R. Bott and C.I. Hussain, 1983, "Studies of Magnetite Deposition from a Flowing Suspension", Chemical Engineering Communications, 20(5-6), pp. 335-353.
[80] C.I. Hussain, I.H. Newson, and T.R. Bott, 1986, "Diffusion Controlled Deposition of Particulate Matter from Flowing Slurries", Heat-transfer 1986: Proceedings of the Eighth International Heat-transfer Conference, San Francisco, California, Volume 5, pp. 2573-2579.
[81] D. Thomas and U. Grigull, 1974, "Experimental Investigation of the Deposition of Suspended Magnetite from the Fluid Flow in Steam Generating Boiler Tubes", Brennstoff-Warme-Kraft, 26(3), pp. 109-115.
[82] I.H. Newson, G.A. Miller, J.W. Haynes, T.R. Bott, and R.D. Williamson, 1988, "Particulate Fouling: Studies of Deposition, Removal and Sticking Mechanisms in a Hematite/Water System", Proceedings for the Second United Kingdom National Conference on Heat-Transfer, Glasgow, Volume 1, pp. 137-160.
[83] R. Williamson, I. Newson and T.R. Bott, 1988, "The Deposition of Haematite Particles from Flowing Water", Canadian Journal of Chemical Engineering, 66(1), pp. 51-54.
[84] R.J. Kuo and E. Matijevic,1981, "Particle Adhesion and Removal in Model Systems. III Monodispersed Ferric Oxide on Steel", Journal of Colloid Interface Science, 78(2), pp. 407-421.

[85] C.W. Turner, D.H. Lister and D.W. Smith, 1990, "The Deposition and Removal of Sub-Micron Particles of Magnetite at the Surface of Alloy 800", Proceedings of the Steam Generator and Heat Exchanger Conference, Toronto, Ontario, Volume 2, 6B-64-6B-76. AECL-10441.
[86] K.A. Burrill, 1977, "The Deposition of Magnetite Particles from High Velocity Water onto Isothermal Tubes", Atomic Energy of Canada Limited Report AECL-5308 1977 February.
[87] N.N. Mankina, 1961, "Formation of Iron Deposits in Recirculation Steam Boilers", British Power Engineering, 2(4), pp. 60-63.
[88] N.N. Mankina and B.L. Koktotv, 1973, "On the Problem of the Mechanism of Formation of Iron Oxide Deposits", Teploenergetika, 9, pp. 15-17.
[89] D.H. Charlesworth, 1970, "The Deposition of Corrrosion Products in Boiling Water Systems", Chemical Engineers Symposium Series 66, Number 104, pp. 21-30. AECL-3883.
[90] F.D. Nicholson and J.V. Sarbutt, 1980, "The Effect of Boiling on the Mass Transfer of Corrosion Products in High Temperature, High Pressure Water Circuits", Corrosion, 36(1), pp. 1-9.
[91] I. Iwahori, T. Mizun and H. Koyama, 1979, "Role of Surface Chemistry in Crud Deposition on Heat-transfer Surface", Corrosion, 35(8), pp. 345-350.
[92] Y. Asakura, M. Kikuchi, S. Uchida and H. Yusa, 1978, "Deposition of Iron Oxide on Heated Surfaces in Boiling Water", Nuclear Science and Engineering, 67(1), pp. 1-7.
[93] Y. Asakura, M. Kikuchi, S. Uchida and H. Yusa, 1979, "Iron Oxide Deposition on Heated Surfaces in Pressurized Boiling Water", Nuclear Science and Engineering, 72(1), pp. 117-120.
[94] M. Basset, J. McInerney, N. Arbeau and D.H. Lister, 2000, "The Fouling of Alloy-800 Heat Exchange Surfaces by Magnetite Particles", Canadian Journal of Chemical Engineering, 78(1), pp. 40-52.
[95] H. Carpentier, L. McCrea, and D.H. Lister, 2001, "Deposition of Corrosion Product Particles onto Heat Exchange Surfaces in Bulk Boiling", Proceedings of the International Conference On Heat Exchanger Fouling, Davos, Switzerland, July 8-13, 2001.
[96] N. Arbeau, W. Cook, and D. Lister, 2004, "The Early Stages of Deposition of Magnetite Particles onto Alloy-800 Heat Exchange Surfaces under Subcooled Boiling Conditions", Proceedings of the 2003 ECI Conference on Heat Exchanger Fouling and Cleaning: Fundamentals and Applications, Santa Fe, New Mexico, May 18-22, 2003, Paper 35, pp. 256-262.
[97] L. Wen and C.A. Melendres, 1998, "On the Mechanism of Hematite Deposition on a Metal Surface Under Nucleate Boiling Conditions", Colloids and Surfaces A: Physicochemical and Engineering Aspects, 132(2-3), pp. 315-319.
[98] C.W. Turner, S.J. Klimas and M.G. Brideau, 1997, "The Effect of Alternative Amines on the Rate of Boiler Tube Fouling", Atomic Energy of Canada Limited Report AECL-11848, 1997 October, Electric Power Research Institute Report EPRI TR-108004.
[99] C.W. Turner, S.J. Klimas and P.L. Frattini, 1988, "Reducing Tube-bundle Deposition with Alternative Amines", Proceedings of the Third International Steam Generator and Heat Exchanger Conference, Toronto, Ontario, Canada, June 1998, pp. 257-273.
[100] C.W. Turner, D.A. Guzonas, and S.J. Klimas, 1999, "Surface Chemistry Interventions to Control Boiler Tube Fouling", AECL-12036 (2000), EPRI Report TR-110083 (1999).
[101] S.J. Klimas, D.A. Guzonas and C.W. Turner, 2002, "Identification and Testing of Amines for Steam Generator Chemistry and Deposit Control", EPRI Report 1002773, December 2002.
[102] S.J. Klimas, K. Fruzzetti, C.W. Turner, P.V. Balakrishnan, G.L. Strati, and R.L. Tapping, 2003, "Identification and Testing of Amines for Steam Generator Corrosion and Fouling Control", 2003 ECI Conference on Heat Exchanger Fouling and Cleaning: Fundamentals and Applications, Santa Fe, New Mexico, May 18-22, 2003, Paper 37, pp. 271-278.
[103] M.A.A. Schoonen, 1994, "Calculation of the Point of Zero Charge of Metal Oxides Between 0 and 350 ºC", Geochimica et Cosmochimica Acta, 58(13), pp. 2845-2851.
[104] S.J. Klimas, Y. Lu, and D. Beaton, 2004, "Identification and Testing of Amines for Steam Generator Chemistry and Deposit Control – Part 3: Qualification of Dodecylamine as an Amine Additive for Steam Generator Fouling Mitigation", EPRI 1011320, November 2004.
[105] P.V. Balakrishnen, S.J. Klimas L. Lepine, and C.W. Turner, 1999, "Polymeric Dispersants for Control of Steam Generator Fouling", Atomic Energy of Canada Limited Report AECL-11975, COG-99-165-I, 1999 May.
[106] P. Burgmayer, R. Crovetto, C. W. Turner and S.J. Klimas, 1999, "Effectiveness of Selected Dispersants on Magnetite Deposition at Simulated PWR Heat-Transfer Surfaces", AECL-11976, 1999 July.
[107] H. Hirano, M. Domae, K. Miyajima and K. Yoneda, 2010, "Study on the Mechanism of Flow-Hole Blockage of Steam Generator Tube-support Plates under PWR Secondary Conditions", Nuclear Plant Chemistry Conference 2010, Quebec City.
[108] H.E.C. Rummens, C.W. Turner and J.T. Rogers, 1997, "The Effect of Tube-Support Design on Steam Generator Fouling Susceptibility", Proceedings of Understanding Heat Exchanger Fouling and Mitigation, Lucca. AECL report FFC-FCT-079P.
[109] T. Prusek, E. Moleiro, F. Oukacine, O. Touazi, M. Grandotto, M. Jaeger and A. Adobes, 2011, "Deposit Model for Tube-support Plate Blockage in Steam Generators", Proceedings of the Fourteenth International Topical Meeting on Nuclear Reactor Thermalhydraulics, Toronto, Ontario.
[110] T.R. Beck, D.W. Mahaffey and J.H. Olsen, 1970, "Wear of Small Orifices by Streaming Current Driven Corrosion", Transactions of the ASME Journal of Basic Engineering, 92(4), pp. 782-788.
[111] I.S. Woolsey, D.M. Thomas, K. Garbett and G.J. Bignold, 1989, "Occurrence and Prevention of Enhanced Oxide Deposition in Boiler Flow Control Orifices", Water Chemistry of Nuclear Reactor Systems 5, Bournemouth, England, Volume 1, pp. 219-228.
[112] J. Robertson, 1986, "Corrosion and Deposition Due To Electrokinetic Currents", Central Electricity Generating Board Report TPRD/L/3030/R86, September.
[113] R.J. Hunter, 1981, "Zeta Potential in Colloid Science: Principles and Applications", Academic Press, New York.
[114] M. Guillodo, P. Combrade, B. dos Santos, T. Muller, G. Berthollon, N. Engler, C. Brun and G. Turluer, 2005, "Formation of Deposits in HT Water Under High Velocity Conditions: A Parametric Study", Proceedings of the International Conference on Water Chemistry of Nuclear Reactor Systems, San Francisco, California, October 2004, EPRI 1011579, pp. 1941-1949.
[115] M. Guillodo, T. Muller, M. Barale, M. Foucault, M-H. Clinard, C. Brun, F. Chahma, G. Corredera and O. de Bouvier, 2009, "Singular Deposit Formation in PWR Due to Electrokinetic Phenomena-Application to SG Clogging", 6th CNS International Steam Generator Conference, Toronto, Ontario, November 8-11, 2009, Paper 4.05.
[116] M. Barale, M. Guillodo, C. Brun, M-H. Clinard, G. Corredera and O. De Bouvier, 2008, "Preliminary Laboratory Tests of Investigation on the Blockage Phenomena Observed on TSP of French SGs", Proceedings of the International Conference on Water Chemistry of Nuclear Reactor Systems, Berlin, Germany, Paper P2-41.
[117] M. Guillodo, M. Barale, M. Foucault, N. Ryckelynck, M-H. Clinard, F. Chahma, C. Brun, and G. Corredera, 2010, "Secondary Side TSP Deposit Buildup: Lab Test Investigation Focus on Electrokinetic Considerations", Nuclear Plant Chemistry Conference 2010 (NPC 2010), Quebec City, Quebec, October 3-7, 2010.
[118] R. Roofthooft, 1990, "Belgian Steam Generator Chemical Cleaning and Related Waste Management", Proceedings of the Steam Generator Sludge Management Workshop, Nashville, Tennessee.
[119] B.L.Dow, 1994, "Overview of Steam Generator Chemical Cleaning Experience", Proceedings: Steam Generator Sludge Management Workshop, Norfolk, Virginia, May 10-12, 1994, EPRI TR-104212, Paper 36.
[120] S. Evans, S. Watson, J. Remark, and C. Hengge, 2002, "Review of Steam Generator Chemical Cleaning Experiences from 1998–2002", Proceedings of the 4th Canadian Nuclear Society International Steam Generator Conference, Toronto, Ontario, Canada, May 5-8, 2002.
[121] C.W. Turner, Y Liner, and M.B. Carver, 1994, "Modelling Magnetite Particle Deposition in Nuclear Steam Generators and Comparisons with Plant Data", Second International Steam Generator and Heat Exchanger Conference, Toronto, Ontario, Canada, June 1994, pp. 4.51-4.64.
[122] C. Welty, 1984, "Steam Generator Needs and Practices: Uses of Data", Proceedings: Workshop on Corrosion Product Sampling From Hot Water Systems, Blacksburg, Virginia, August 18-19, 1983, Electric Power Research Institute Report EPRI NP-3402-SR, pp. 5-1 – 5-11.

[123] M. Chocron, N. Fernandez and J.A. Sawicki, 1999, "Crud Transport and Sludge Control at Embalse", Proceedings: Steam Generator Sludge Management Workshop, Scottsdale, Arizona, September 30-October 1, 1999, EPRI TR-114854, Paper 5-1.
[124] C. Marks, 2009, "Steam Generator Management Program: Effects of Different pH Control Agents on Pressurized Water Reactor Plant Systems and Components", Electric Power Research Institute Report 1019042.
[125] J.J. Schuck, C.C. Nathan and J.R. Metcalf, 1973, "Corrosion Inhibitors for Steam Condensate Systems", Materials Protection and Performance, 12(10), pp. 42-47.
[126] M.F. Obrecht, 1964, "Steam and Condensate Return Line Corrosion – How to Employ Filming Amines for its Control", Heating, Piping and Air Conditioning, pp. 116-122.
[127] A.A. Avdeev, A.N. Kukushkin, D.A. Repin, V.V. Omelchuk, L.F. Barmin, V.A. Yurmanov and E. Czempik, 2010, "The Impact of ODA Microadditions into Secondary System on Corrosion Rate Reduction in VVER Steam Generators", Nuclear Plant Chemistry Conference 2010 (NPC 2010), Quebec City, Quebec, October 3-7, 2010.
[128] J. Fandrich, S. Hoffmann-Wankel, U. Ramminger, and B. Stellwag, 2012, "pH Optimization Strategy and Application of Film Forming Amines in the Secondary Side Chemistry Treatment of NPPs", Proceedings: Steam Generator Management Program, 2012 Steam Generator Secondary Side Management Conference, Atlanta, Georgia, EPRI 1026545, pp. 2-344 – 2-386.
[129] U. Ramminger, S. Hoffmann-Wankel, and J. Fandrich, 2012, "The Application of Film Forming Amines in Secondary Side Chemistry Treatment of NPPs", Nuclear Plant Chemistry Conference 2012 (NPC 2012), Paris, France. (Also published in: Revue Generale Nucleaire, no.6, 2012, pp. .68-73)
[130] K. Fruzzetti, P. Frattini, P. Robbins, A. Miller, R. Varrin and M. Kreider, 2002, "Dispersant Trial at ANO-2: Results from a Short-Term Trial Prior to SG Replacement", International Conference on Water Chemistry in Nuclear Reactor Systems, Avignon, France, April 2002.
[131] K. Fruzzetti, P. Frattini, P. Robbins, A. Miller, R. Varrin, and M. Kreider, 2002, "Dispersant Trial at ANO-2: Results From a Short-Term Trial Prior to SG Replacement", International Conference on Water Chemistry in Nuclear Reactor Systems, Avignon, France, April 2002.
[132] K. Fruzzetti, D. Rochester, L. Wilson, M. Kreider and A. Miller, 2008, "Dispersant Application for Mitigation of Steam Generator Fouling: Final Results from the McGuire 2 Long-Term Trial and an Industry Update and EPRI Perspective for Long-Term Use", International Conference on Water Chemistry of Nuclear Reactor Systems, Berlin, Germany, September 15-18, 2008.
[133] K. Fruzzetti, S. Choi, C. Haas, M. Pender and D. Perkins, 2010, "PWR Chemistry Controls: A Perspective on Industry Initiatives and Trends Relative to Operating Experience and the EPRI PWR Water Chemistry Guidelines", Nuclear Plant Chemistry Conference 2010 (NPC 2010), Quebec City, Quebec, October 3-7, 2010.
[134] K. Fruzzetti, C. Anderson, C. Marks, M. Kreider, B. Walton, W. Reecher and D. Morey, 2010, "Dispersant Application: (1) During Steam Generator Wet Layup for Removal of Existing Deposits, and (2) During the Long-Path Recirculation Cleanup Process of the Condensate/Feedwater System to Reduce Startup Corrosion Product Transport to the Steam Generators", Nuclear Plant Chemistry Conference 2010 (NPC 2010), Quebec City, Quebec, October 3-7, 2010.
[135] "Standards of the Tubular Exchanger Manufacturers Association", First Edition, TEMA, New York (1941).